Computational Biology in the Petascale Era

Advancing the Computational Microscope

Accuracy • Speed-up • Unprecedented Scale

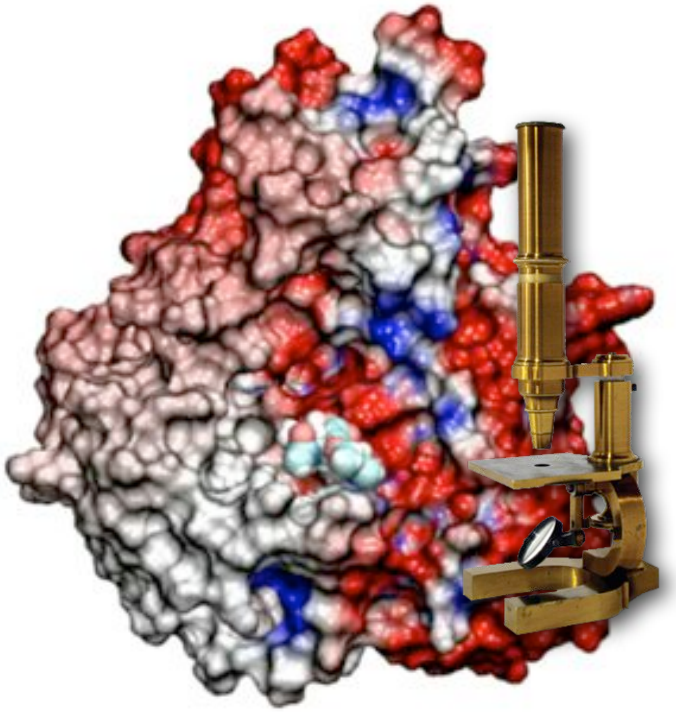

Investigation of drug (Tamiflu) resistance of the "swine" flu virus

Klaus Schulten

Department of Physics and

Theoretical and Computational Biophysics Group

University of Illinois at Urbana-Champaign

Lecture at. U. Tennesee and ORNL, April 2012

Our Microscope is Made of...

Chemistry

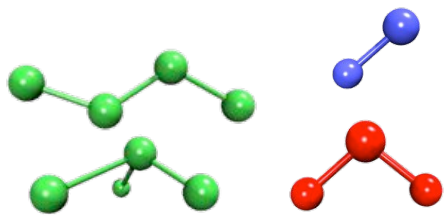

$$U(\vec{R}) = \underbrace{\sum_{bonds} k_i^{bond}(r_i - r_0)^2}_{U_{bond}} + \underbrace{\sum_{angles} k_i^{angle}(\theta_i - \theta_0)^2}_{U_{angle}} + \underbrace{\sum_{dihedrals} k_i^{dihe}[1 + \cos(n_i\phi_i + \delta_i)]}_{U_{dihedral}} + \underbrace{\sum_i \sum_{j \neq i} 4\epsilon_{ij}\left[\left(\frac{\sigma_{ij}}{r_{ij}}\right)^{12} - \left(\frac{\sigma_{ij}}{r_{ij}}\right)^{6}\right] + \sum_i \sum_{j \neq i} \frac{q_i q_j}{\epsilon r_{ij}}}_{U_{nonbond}}$$

NAMD Software

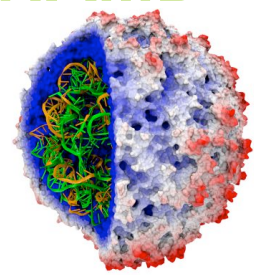

Virus

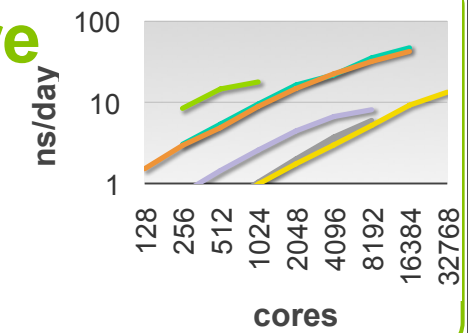

Physics

$$m_i \frac{d^2\vec{r}_i}{dt^2} = \vec{F}_i = -\vec{\nabla} U(\vec{R})$$

Math

$$\vec{r}_i(t + \Delta t) = 2\vec{r}_i(t) - \vec{r}_i(t - \Delta t) + \frac{\Delta t^2}{m_i}\vec{F}_i(t)$$

(repeat ***one billion times*** = microsecond)

..and Supercomputers

NAMD impact is broad and deep

- Comprehensive, industrial-quality software
  - Integrated with VMD for simulation setup and analysis
  - Portable extensibility through Tcl scripts (also used in VMD)
  - Consistent user experience from laptop to supercomputer
- Large user base – 51,000 registered users
  - 9,100 (18%) are NIH-funded; many in other countries
  - 14,100 have downloaded more than one version
- Leading-edge simulations
  - "most-used software" on NICS Cray XT5 (largest NSF machine)
  - "by far the most used MD package" at TACC (2nd and 3rd largest)
  - NCSA Blue Waters early science projects and acceptance test
  - Argonne Blue Gene/Q early science project

Outside researchers choose NAMD and succeed

2100 external citations since 2007

Corringer, et al., *Nature*, 2011

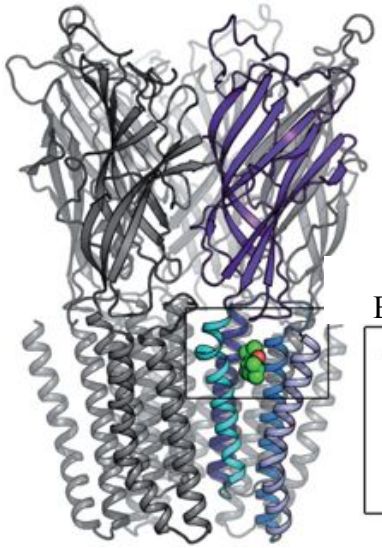

180K-atom 30 ns study of anesthetic binding to bacterial ligand-gated ion channel provided "complementary interpretations…that could not have been deduced from the static structure alone."

Bound Propofol Anesthetic

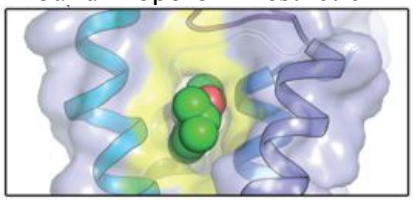

Voth, et al., *PNAS*, 2010

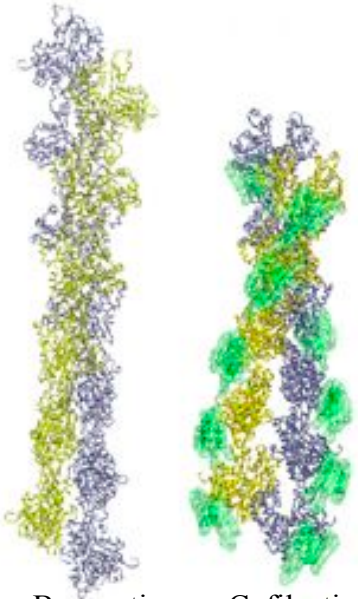

Bare actin Cofilactin

500K-atom 500 ns investigation of effect of actin depolymerization factor/cofilin on mechanical properties and conformational dynamics of actin filament.

Recent NAMD Simulations in *Nature*

- **M. Koeksal, et al.,** *Taxadiene synthase structure and evolution of modular architecture in terpene biosynthesis*. (2011)
- **C.-C. Su, et al.**, *Crystal structure of the CusBA heavy-metal efflux complex of Escherichia coli.* (2011)
- **D. Slade, et al.**, *The structure and catalytic mechanism of a poly(ADP-ribose) glycohydrolase*. (2011)
- **F. Rose, et al.,** *Mechanism of copper(II)-induced misfolding of Parkinson's disease protein*. (2011)
- **L. G. Cuello, et al.**, *Structural basis for the coupling between activation and inactivation gates in K(+) channels*. (2010)
- **S. Dang, et al.,**, *Structure of a fucose transporter in an outward-open conformation.* (2010)
- **F. Long, et al.**, *Crystal structures of the CusA efflux pump suggest methionine-mediated metal transport*. (2010)
- **R. H. P. Law, et al.**, *The structural basis for membrane binding and pore formation by lymphocyte perforin.* (2010)
- **P. Dalhaimer and T. D. Pollard**, *Molecular Dynamics Simulations of Arp2/3 Complex Activation.* (2010)
- **J. A. Tainer, et al.**, *Recognition of the Ring-Opened State of Proliferating Cell Nuclear Antigen by Replication Factor C Promotes Eukaryotic Clamp-Loading*. (2010)
- **D. Krepkiy, et al.,**, *Structure and hydration of membranes embedded with voltage-sensing domains*. (2009)
- **N. Yeung, et al.,**, *Rational design of a structural and functional nitric oxide reductase*. (2009)
- **Z. Xia, et al.**, *Recognition Mechanism of siRNA by Viral p19 Suppressor of RNA Silencing: A Molecular Dynamics Study*. (2009)

Computing Research Drives NAMD

- Parallel Programming Lab – (Laxmikant Kale)
  - Charm++ is an Adaptive Parallel Runtime System
    - Gordon Bell Prize 2002
    - Three publications at Supercomputing 2011
    - Four panels discussing the future necessity of our ideas
- 20 years of co-design for NAMD performance, portability, and productivity, adaptivity
    - Recent example: Implicit Solvent deployed in NAMD by 1 RA in 6 months. 4x more scalable than similar codes
- Yesterday's supercomputer is tomorrow's desktop

Highly Scalable as Seen in Case of Implicit Solvent Model

NAMD Implicit Solvent is 4x more scalable than Traditional Implicit Solvent for all system sizes; implemented by a graduate student in 6 months.

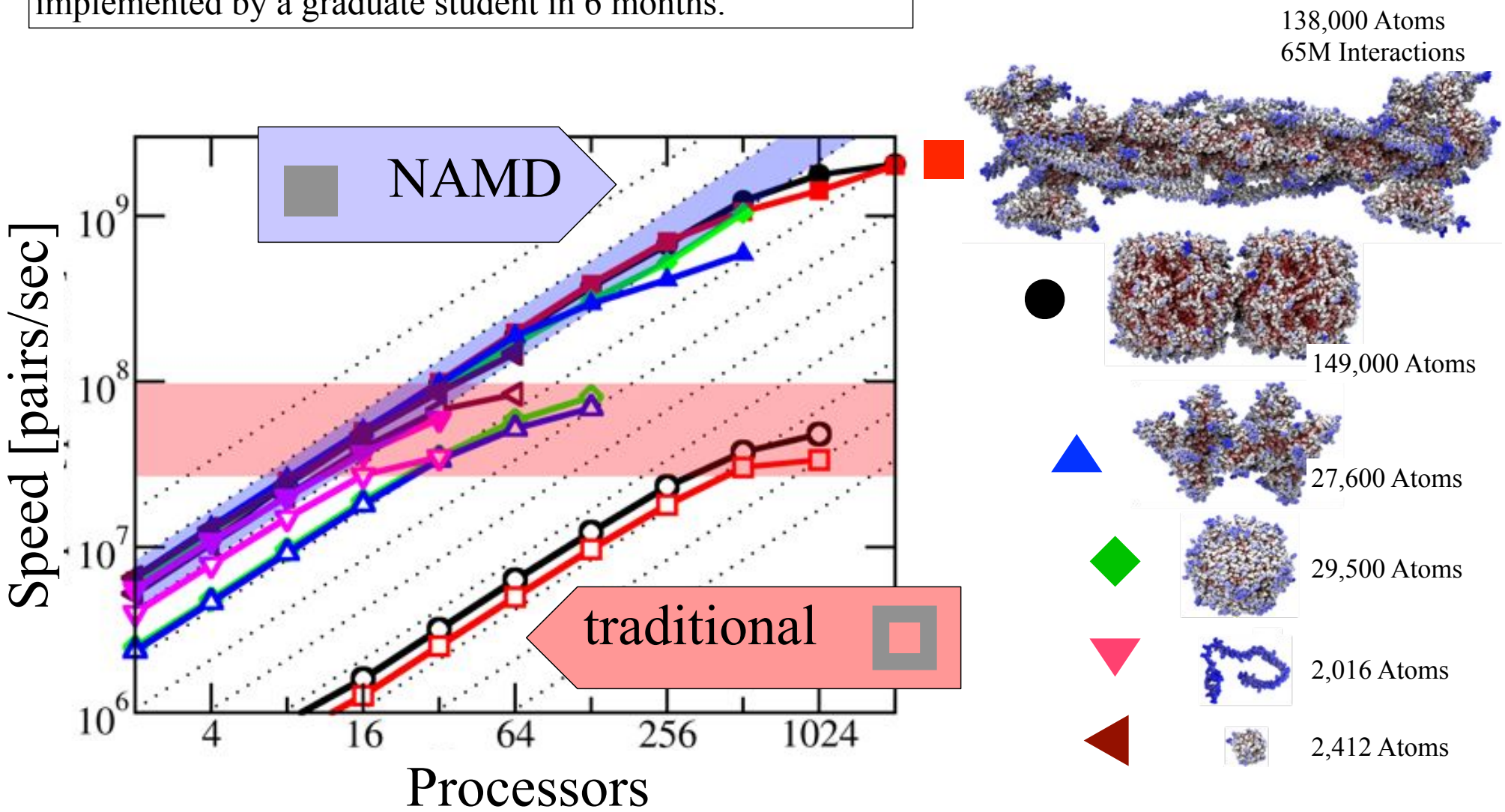

Tanner et al., J. Chem. Theory and Comp., 7:3635-3642, 2011

Improving Force Field: Atomic Polarizability

- Atomic polarizability increases computation by 2x…
- …but, the additional computations are perfectly suited to the GPU!
- For now, NAMD calculates atomic polarizability on CPUs only...soon we will also use GPUs

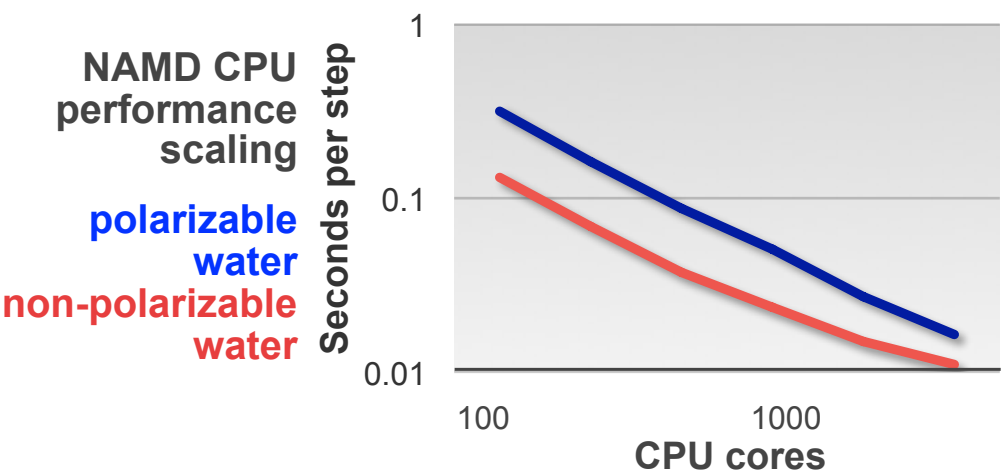

Atomic polarizability of water, highly accurately simulated through additional particles (shown in green)

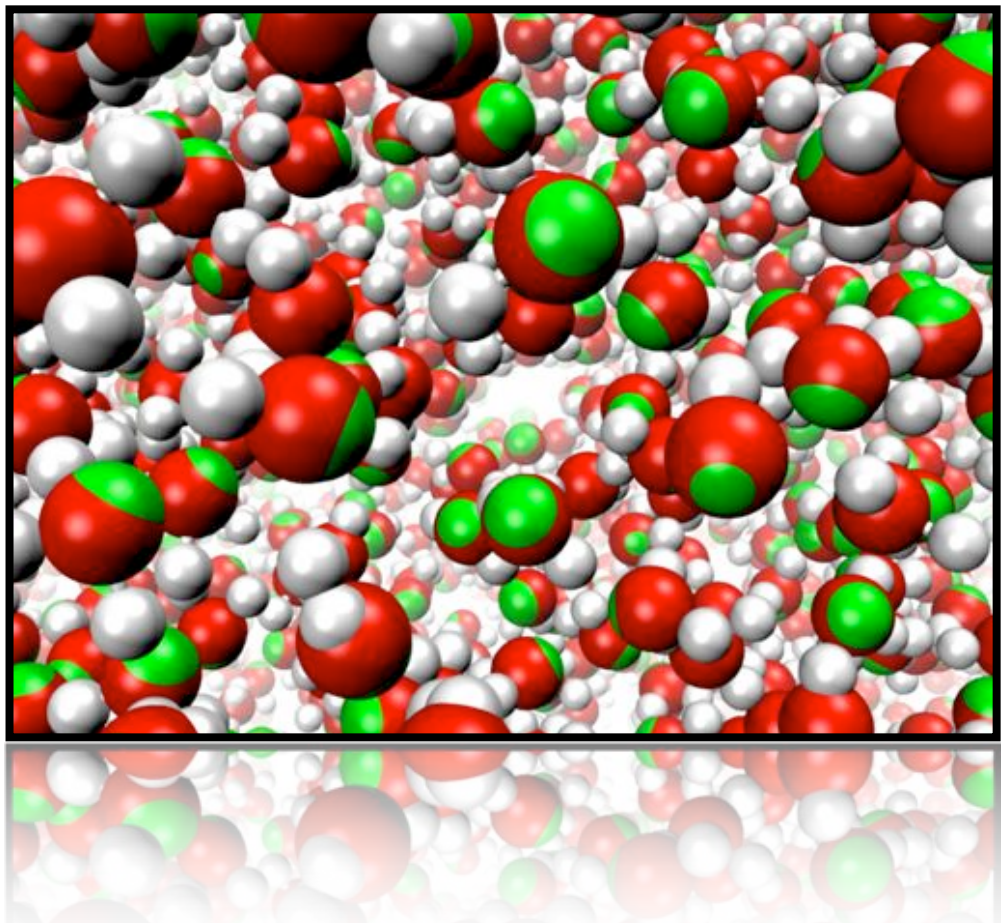

Works equally well for Drude and Fluctuating Charge Force Field;! Support of Amoeba force field planned.

Computational Microscope on New Supercomputers

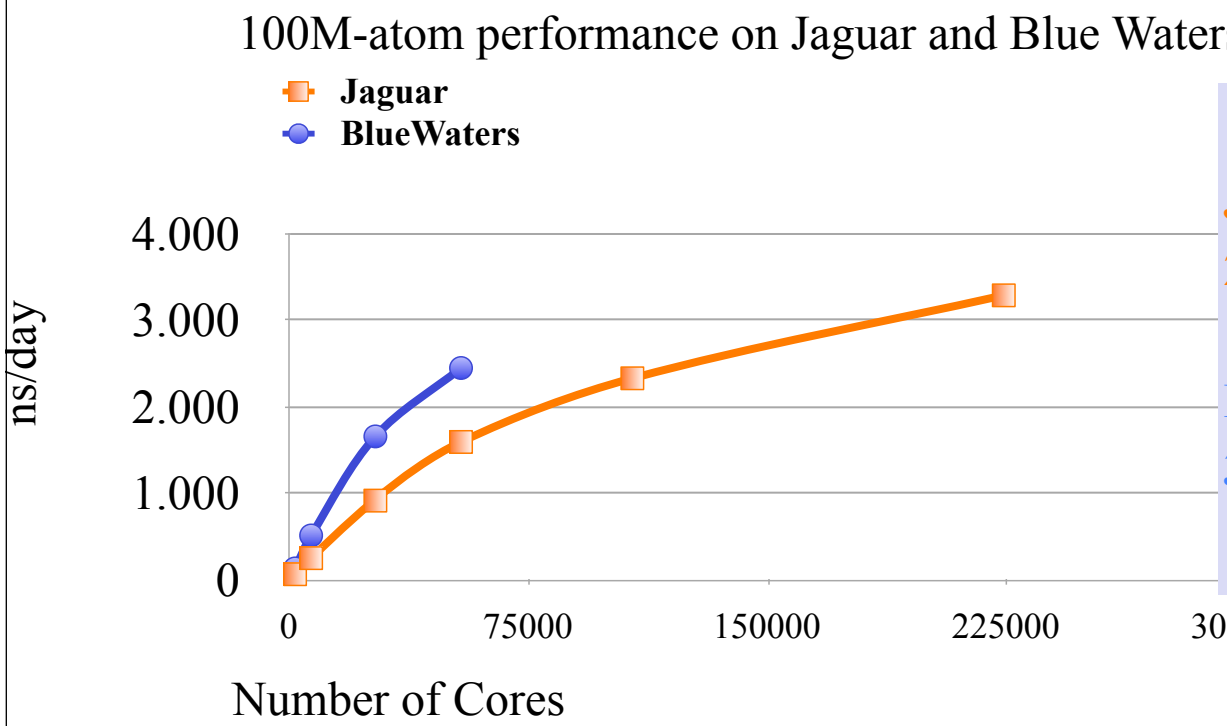

Cray

Jaguar XT5 (ORNL)
224,000 cores

BlueWaters XE6 (UIUC)
380,000 cores, 3000 GPUs

Tsubame

Tokyo Institute of Tech.
4224 GPUs

50,000 registered users

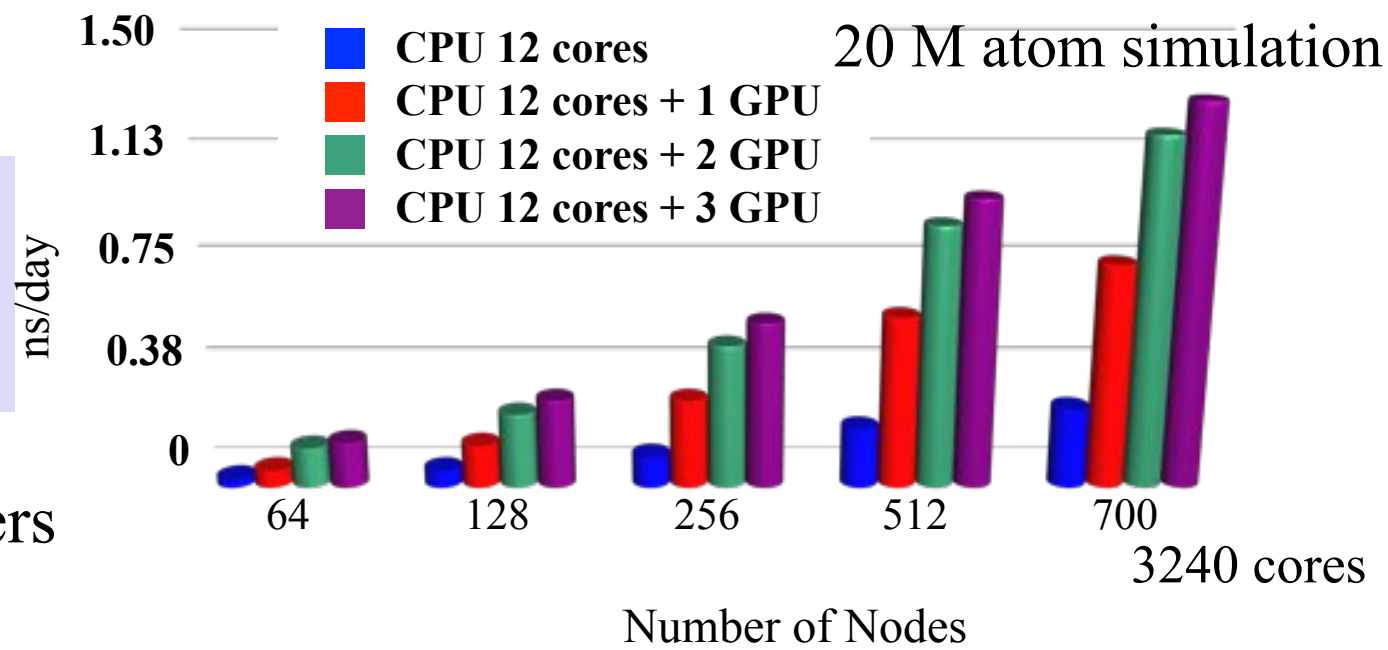

100M Atoms on Titan vs Jaguar

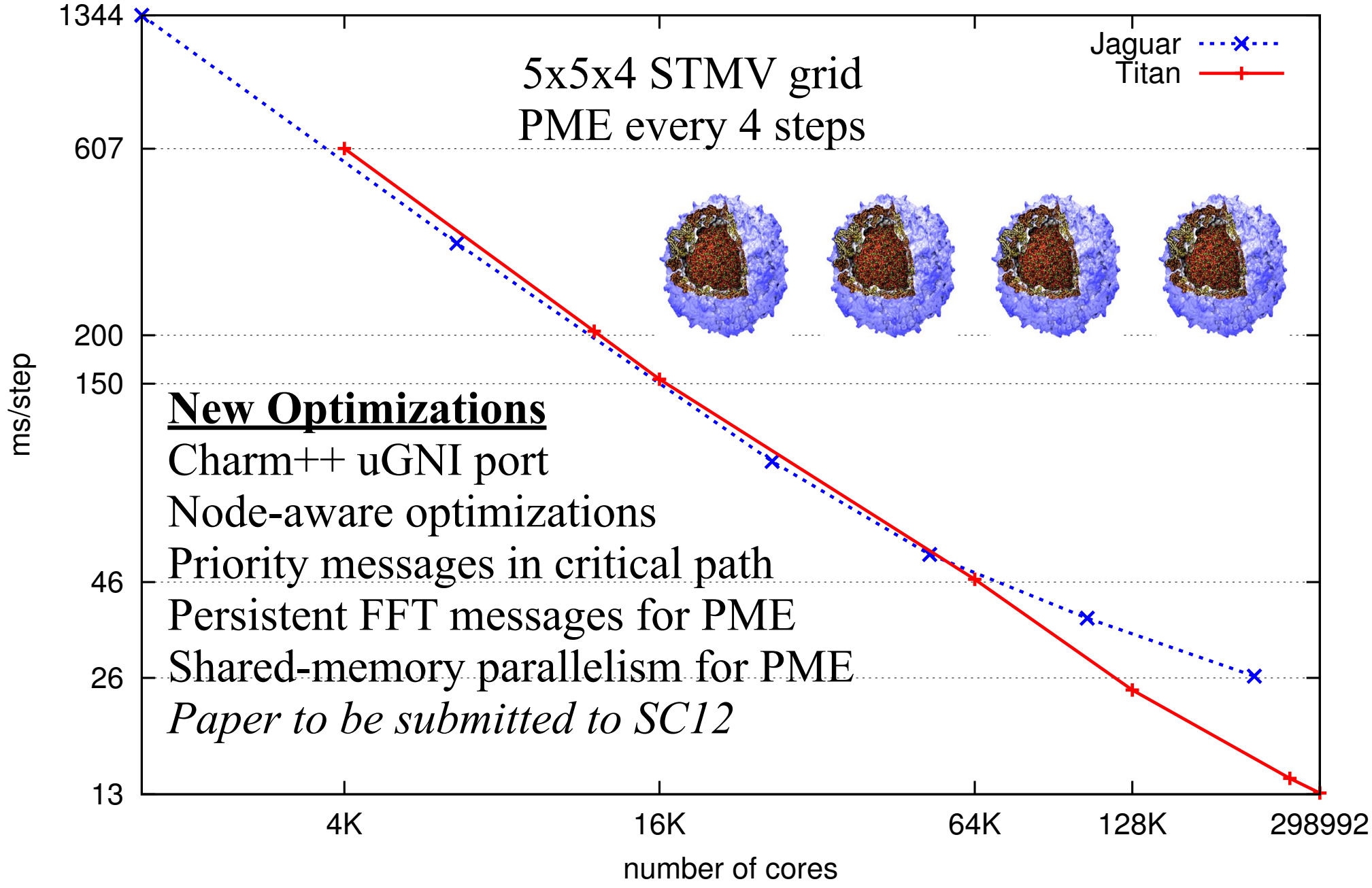

New Optimizations

Charm++ uGNI port

Node-aware optimizations

Priority messages in critical path

Persistent FFT messages for PME

Shared-memory parallelism for PME

Paper to be submitted to SC12

1M Atom Virus on TitanDev GPU

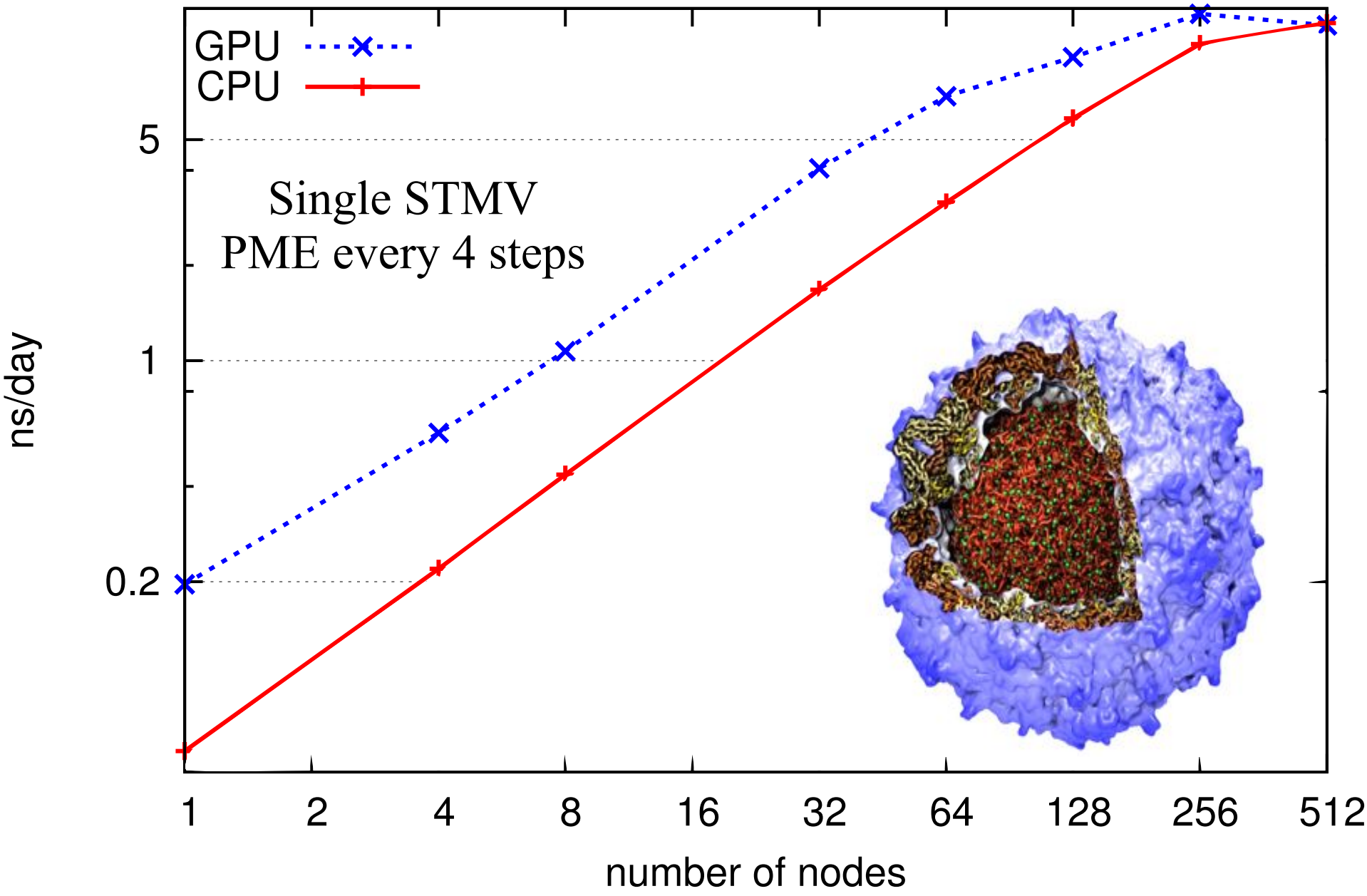

100M Atoms on TitanDev

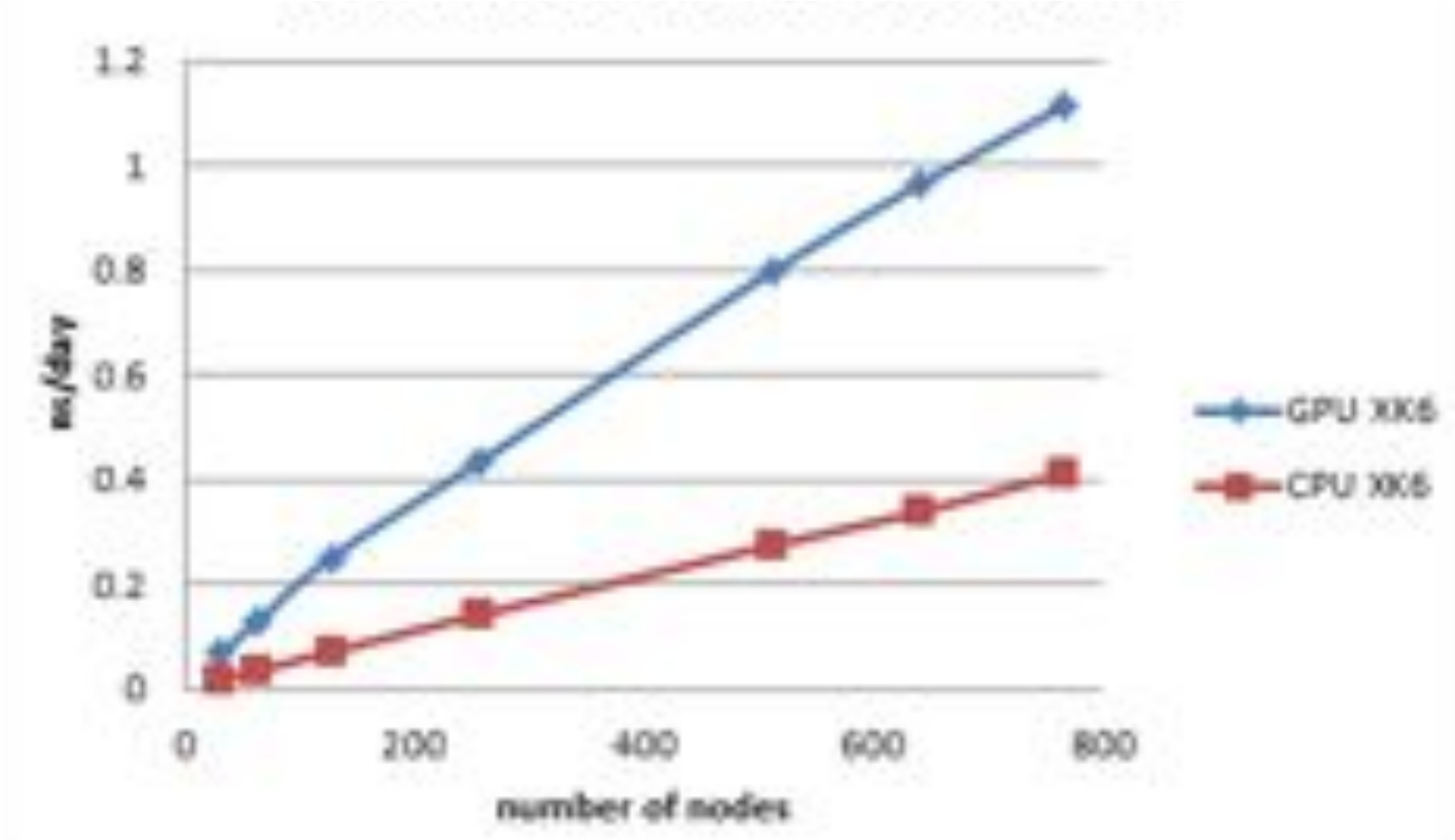

TitanDev Cray XK6 Results

	100 stmv s/step 32 nodes	100 stmv s/step 768 nodes
XK6, Fermi	1.23065 s	0.07657 s
XK6, without Fermi	4.62633 s	0.19688 s
XE6	2.318 s	0.10602 s
XK6 Fermi vs XK6 without Fermi	3.8 x	2.6 x
XK6 Fermi vs XE6	1.8 x	1.4 x

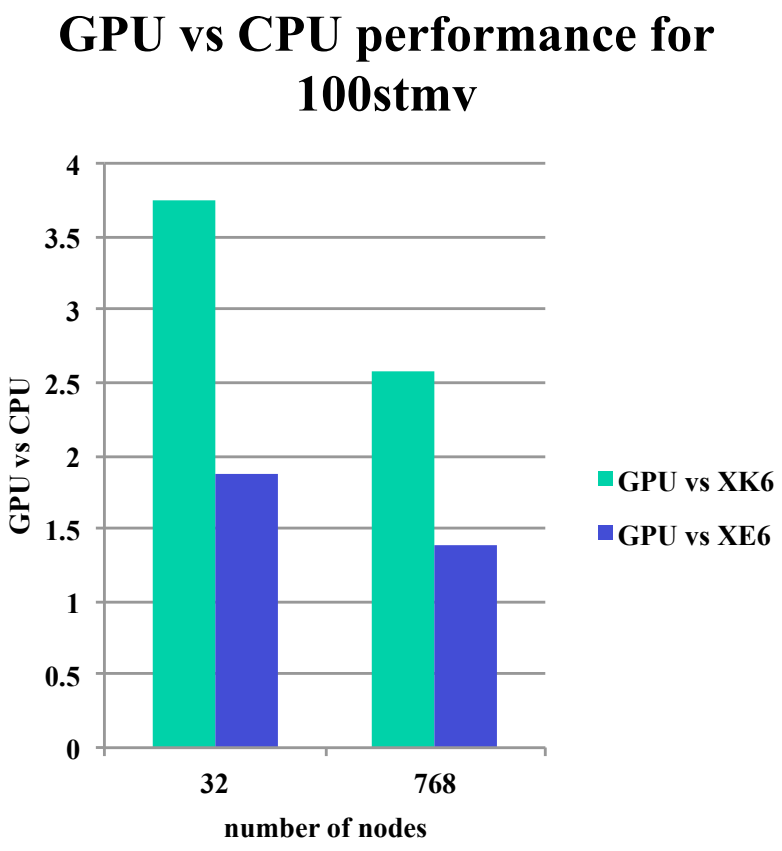

Our Microscope is a "Tool to Think"

Carl Woese

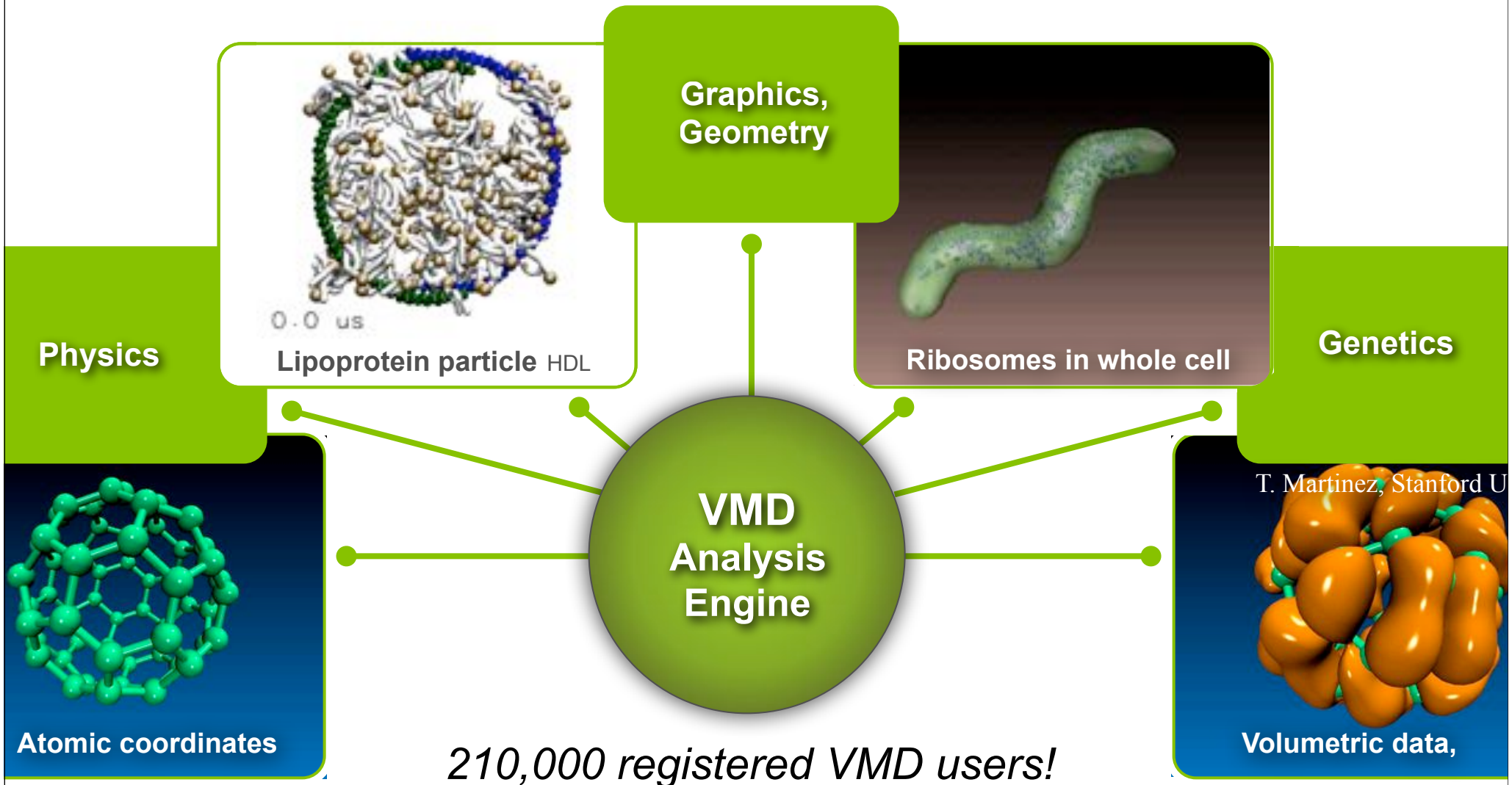

210,000 registered VMD users!

VMD 1.9.1: "QuickSurf" Representation

- Displays continuum of structural detail:
  - All-atom models
  - Coarse-grained models
  - Cellular scale models
  - Multi-scale models: All-atom + CG, Brownian + Whole Cell
  - Smoothly variable between full detail, and reduced resolution representations of very large complexes
- Uses multi-core CPUs and GPU acceleration to enable **smooth real-time animation** of MD trajectories
- Linear-time algorithm, scales to hundreds of millions of particles, as limited by memory capacity

Fast Visualization of Gaussian Density Surfaces for Molecular Dynamics and Particle System Trajectories.
M. Krone, J. Stone, T. Ertl, K. Schulten. *EuroVis* 2012. (*in press*)

GPU Accelerated Trajectory Analysis and Visualization in VMD

GPU-Accelerated Feature	GPU Speedup
Molecular orbital display	120x
Radial distribution function	92x
Electrostatic field calculation	44x
Molecular surface display	40x
Ion placement	26x
MDFF density map synthesis	26x
Implicit ligand sampling	25x
Root mean squared fluctuation	25x
Radius of gyration	21x
Close contact determination	20x
Dipole moment calculation	15x

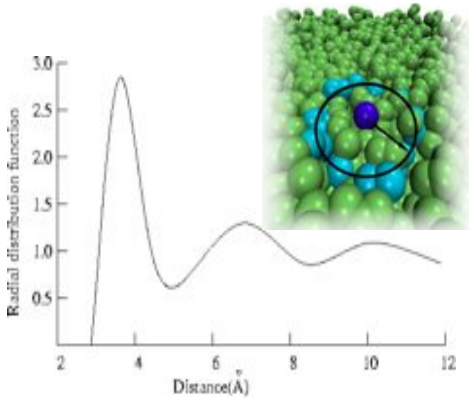

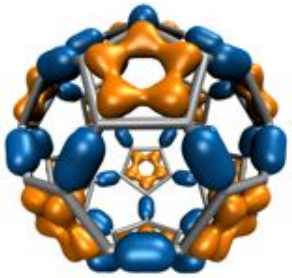

Selected VMD Plugins: Center Developed, and User Developed

Analysis

- APBSRun
- CatDCD
- Contact Map
- GofRGUI
- HeatMapper
- ILSTools
- IRSpecGUI
- MultiSeq
- NAMD Energy
- NAMD Plot
- NetworkView
- NMWiz
- ParseFEP
- PBCTools
- PMEpot
- PropKa GUI
- RamaPlot
- RMSD Tool
- RMSD Trajectory Tool
- RMSD Visualizer Tool
- Salt Bridges
- Sequence Viewer
- Symmetry Tool
- Timeline
- VolMap

Modeling

- AutoIonize
- AutoPSF
- Chirality
- Cionize
- Cispeptide
- CGTools
- Dowser
- ffTK
- Inorganic Builder
- MDFF
- Membrane
- Merge Structs
- Molefacture
- Mutator
- Nanotube
- Paratool
- Psfgen
- RESPTool
- RNAView
- Solvate
- SSRestraints
- Topotools

Visualization

- Clipping Plane Tool
- Clone Rep
- DemoMaster
- Dipole Watcher
- Intersurf
- Navigate
- NavFly
- MultiMolAnim
- Color Scale Bar
- Remote
- Palette Tool
- ViewChangeRender
- ViewMaster
- Virtual DNA Viewer
- VMD Movie Maker

Simulation

- AutoIMD
- IMDMenu
- NAMD GUI
- NAMD Server
- QMTool

68 MolFile I/O Plugins:

structure, trajectory, sequence, and density map

Collaboration

- BioCoRE Chat
- BioCoRE Login
- BioCoRE VMD Shared Views
- Remote Control

Data Import and Plotting

- Data Import
- Multiplot
- PDBTool
- MultiText

Externally Hosted Plugins and Extensions

- Check sidechains
- MultiMSMS
- Interactive Essential Dynamics
- Mead Ionize
- Clustering Tool
- iTrajComp
- Swap RMSD
- Intervor
- SurfVol
- vmdICE

http://www.ks.uiuc.edu/Research/vmd/plugins/

Time-Averaged Electrostatics Analysis on Energy-Efficient GPU Cluster

- **1.5 hour** job (CPUs) reduced to **3 min** (CPUs+GPU)
- Electrostatics of thousands of trajectory frames averaged
- Per-node power consumption on NCSA "AC" GPU cluster:
  - CPUs-only: 299 watts
  - CPUs+GPUs: 742 watts
- GPU Speedup: **25.5x**
- Power efficiency gain: **10.5x**

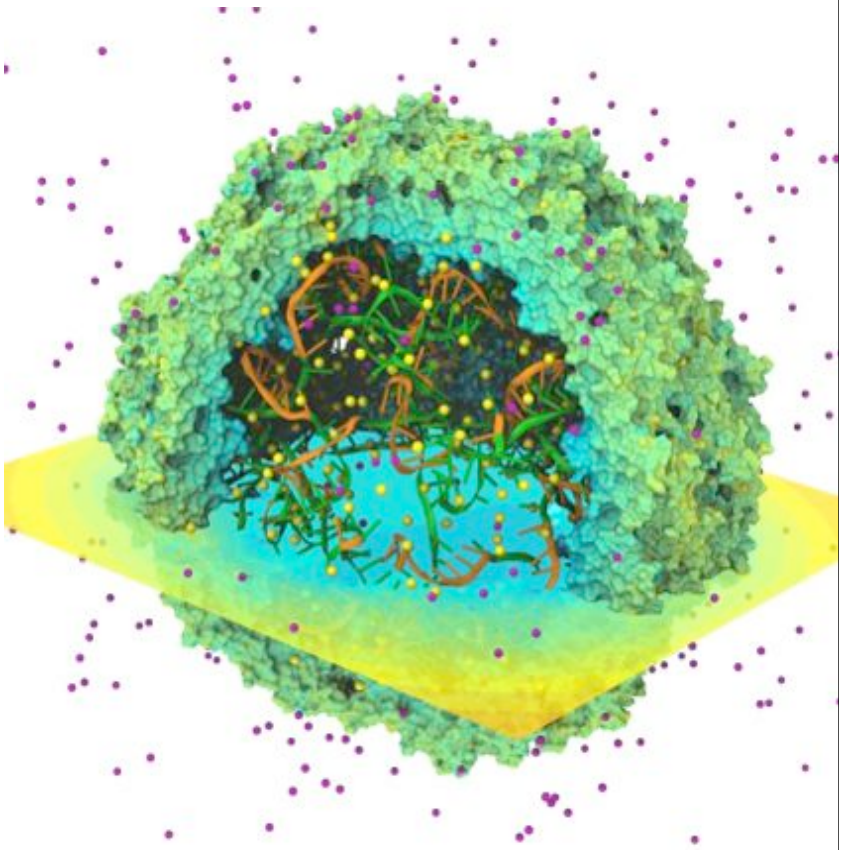

Quantifying the Impact of GPUs on Performance and Energy Efficiency in HPC Clusters. J. Enos, C. Steffen, J. Fullop, M. Showerman, G. Shi, K. Esler, V. Kindratenko, J. Stone, J. Phillips. *The Work in Progress in Green Computing,* pp. 317-324, 2010.

Time-Averaged Electrostatics Analysis on NCSA Blue Waters Early Science System

NCSA Blue Waters Node Type	**Seconds per trajectory frame for one compute node**
Cray XE6 Compute Node: 32 CPU cores (2xAMD 6200 CPUs)	9.33
Cray XK6 GPU-accelerated Compute Node: 16 CPU cores + **NVIDIA X2090 (Fermi) GPU**	2.25
Speedup for GPU XK6 nodes vs. CPU XE6 nodes	**GPU nodes are 4.15x faster overall**

Preliminary performance for VMD time-averaged electrostatics w/ Multilevel Summation Method running Blue Waters Early Science System

VMD Out-of-Core Trajectory I/O Performance: SSD-Optimized Trajectory Format, 8-SSD RAID

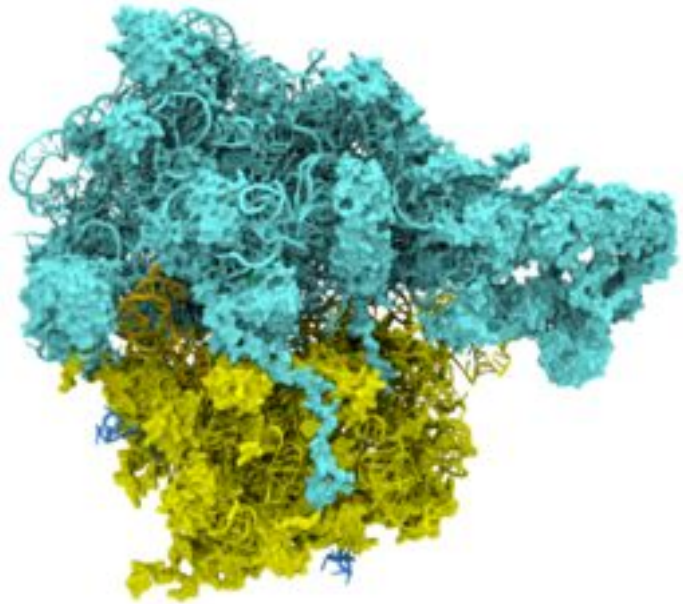

Ribosome w/ solvent
3M atoms
3 frames/sec w/ HD
60 frames/sec w/ SSDs

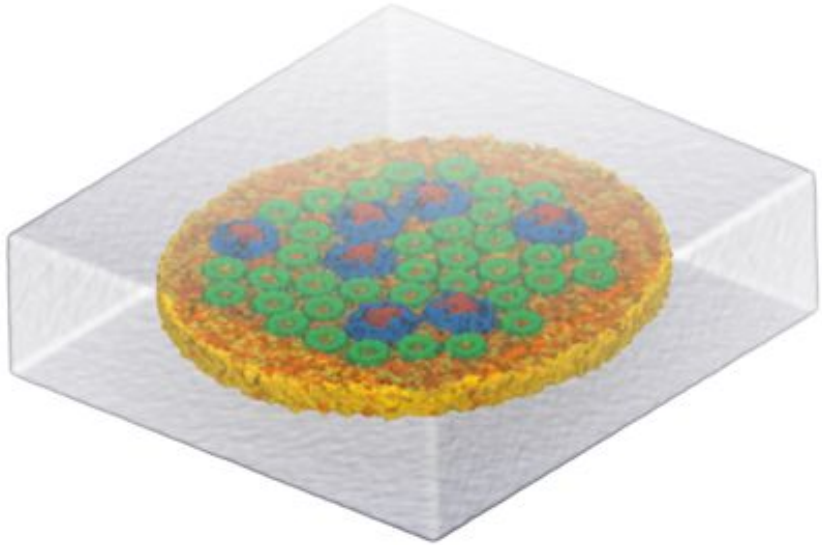

Membrane patch w/ solvent
20M atoms
0.4 frames/sec w/ HD
8 frames/sec w/ SSDs

New SSD Trajectory File Format 2x Faster vs. Existing Formats
VMD I/O rate ~2.1 GB/sec w/ 8 SSDs

Successful folding of largest fast-folding protein: λ-repressor / Collaboration Gruebele-Schulten

System:
- 5-helix bundle protein
- **Largest** fast-folding protein
- Experimental folding time < 20 μs

Yanxin Liu, Johan Strümpfer, Peter L. Freddolino, Martin Gruebele, and Klaus Schulten. **Structural characterization of λ-repressor folding from all-atom molecular dynamics simulations.** *Journal of Physical Chemistry Letters*, **3:**1117-1123, 2012.

Recent progress:
- Successful folding in < 5 μs using enhanced sampling
- 100-μs folding trajectory using both NAMD and Anton

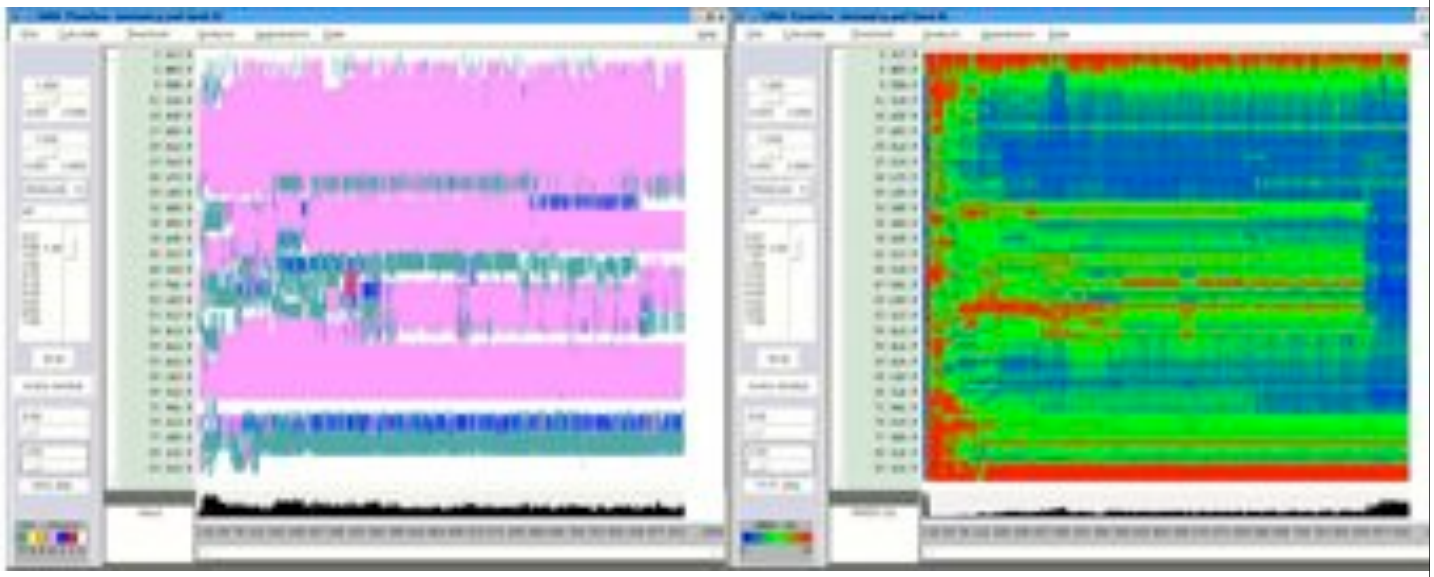

Alpha helix Pi-helix 3-10 helix
Turn None (coil)

Lamda repressor folding, 24.1 μs. Per-residue secondary structure and RMSD.

VMD 1.9.1: New Tablet/Phone Interface

- Developed first multi-touch, multi-user, wireless user interface for VMD
  - Early technology development in advance of devices
- New wireless control using VMD remote control app:
  - Multi-touch input and control of VMD session, scripts, plugins
  - Collaborative multi-user interaction
- Recent: tablet display of trajectory timelines, sequence data, plots, and tabular information
- Goal: tablet-native VMD by end of funding period, w/ simplified graphical user interface

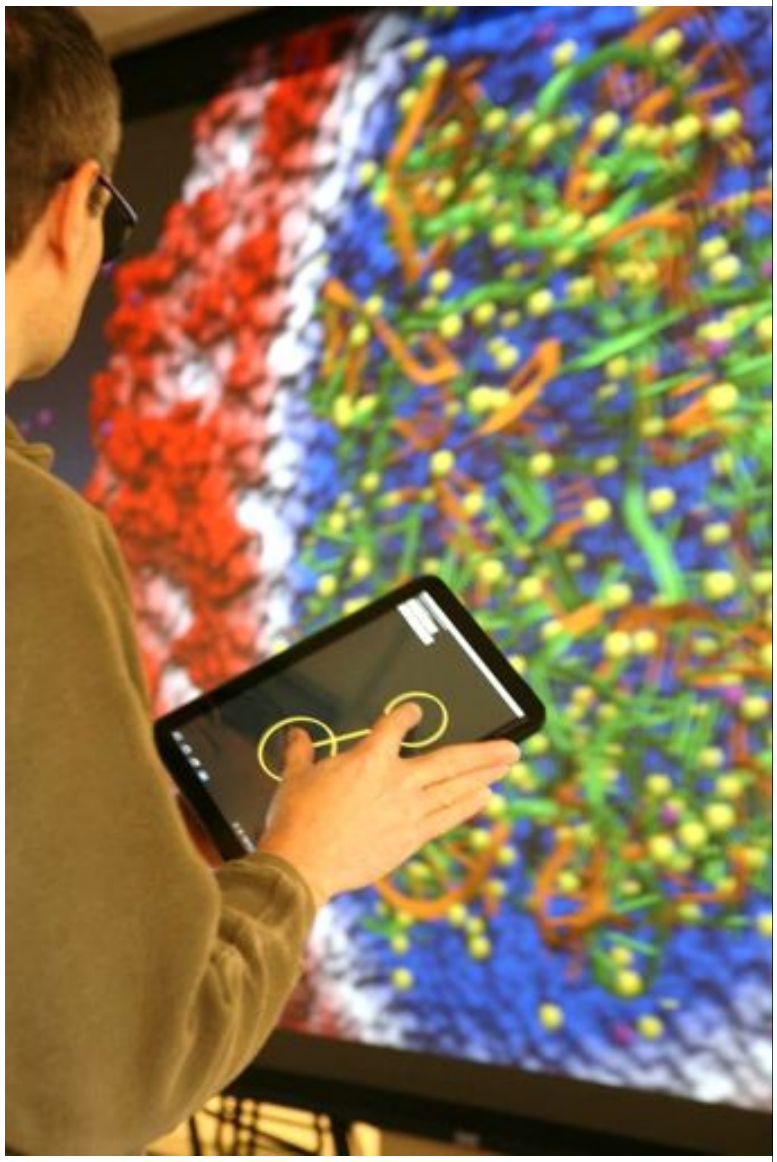

Petascale Gateway, our Key Hardware Component

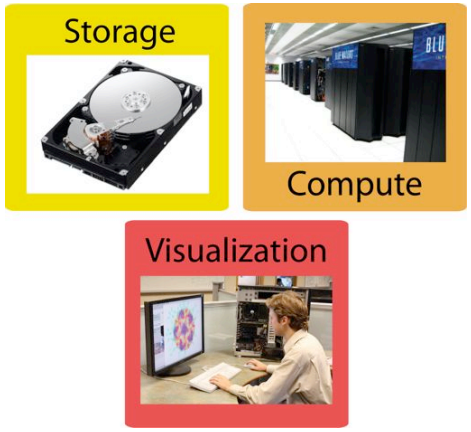

Petascale computers (e.g., Blue Waters) will create ~100x larger datasets. The BTRC Petascale Gateway provides the necessary storage and analysis facilities all located in the BTRC area.

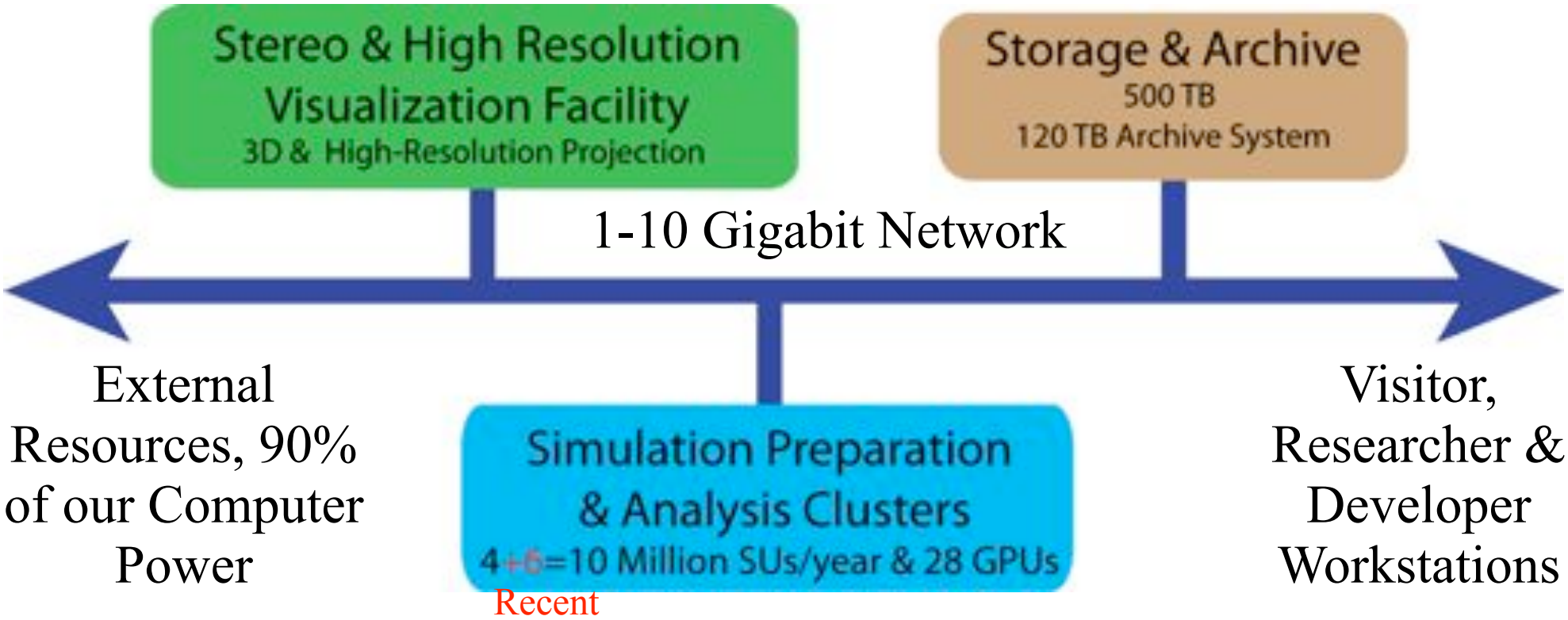

Imaging Cellular Machines

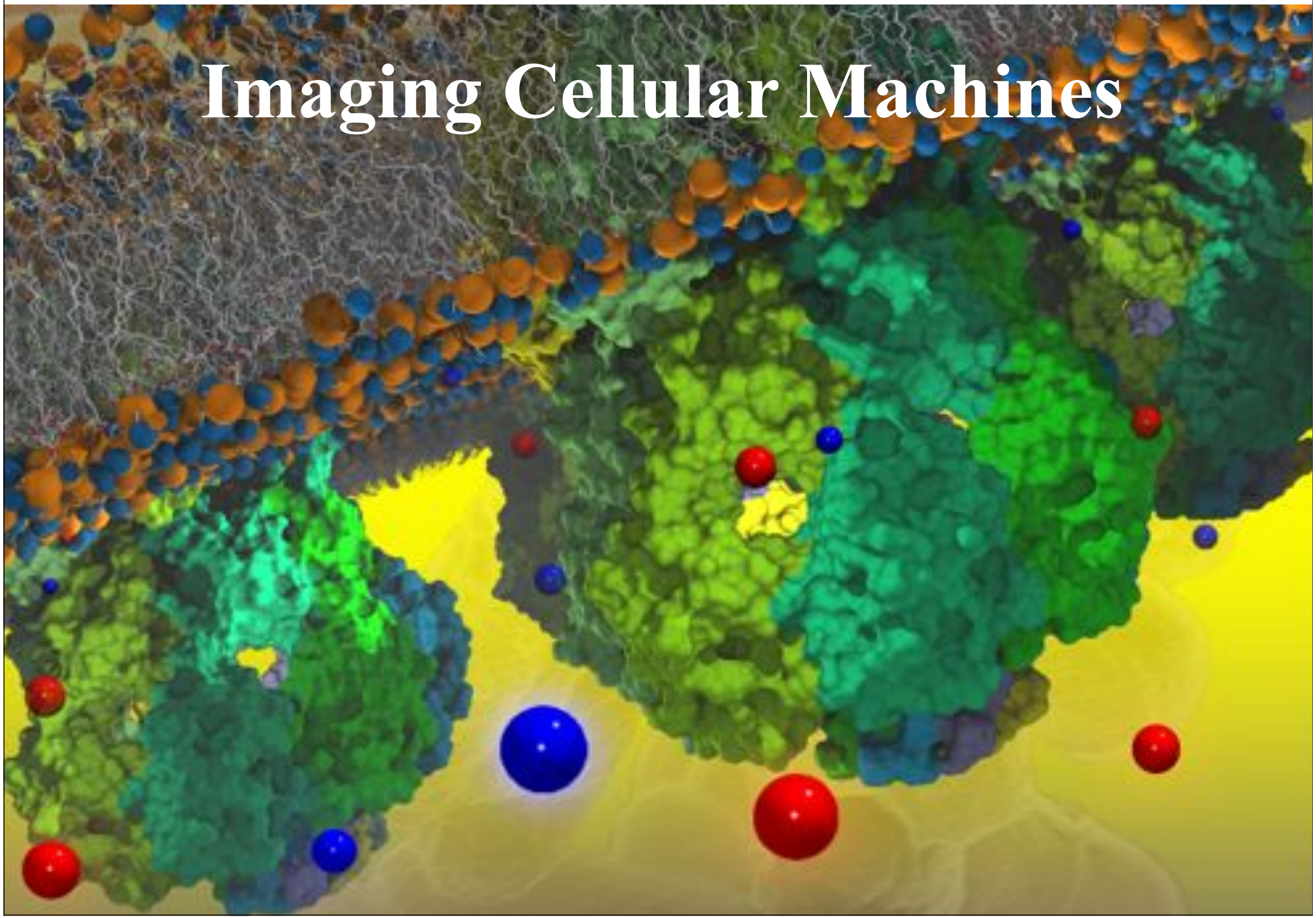

We Employ Classical Mechanics and Quantum Chemistry Methods

Photoactivation Reaction in Photoreceptor Cryptochrome

- Investigated cryptochrome photoactivation using **quantum chemistry**.
- Revealed transient states in cryptochrome post-light-activation using **perturbation theory** for cryptochrome's active site.
- Studied **electron and proton transfer** processes in cryptochrome at the atomic level.
- Performed **QM/MM** calculations for selected transient states of cryptochrome.

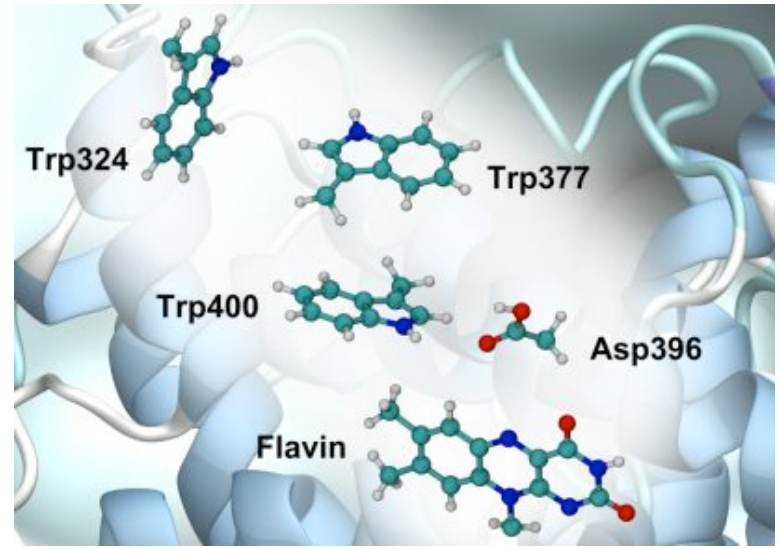

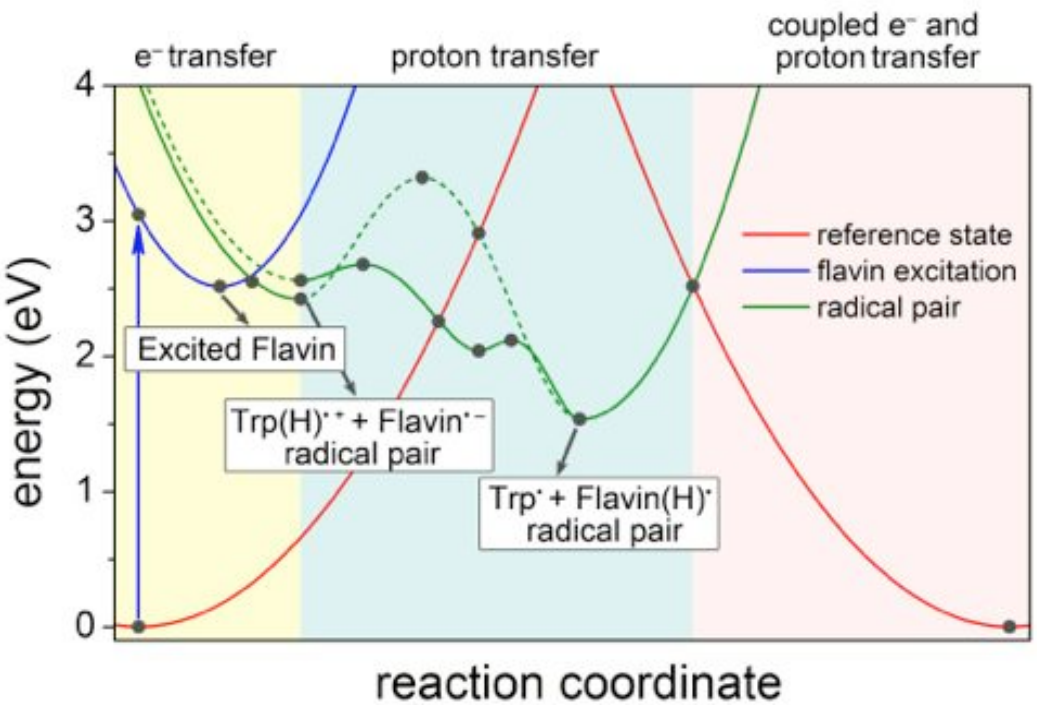

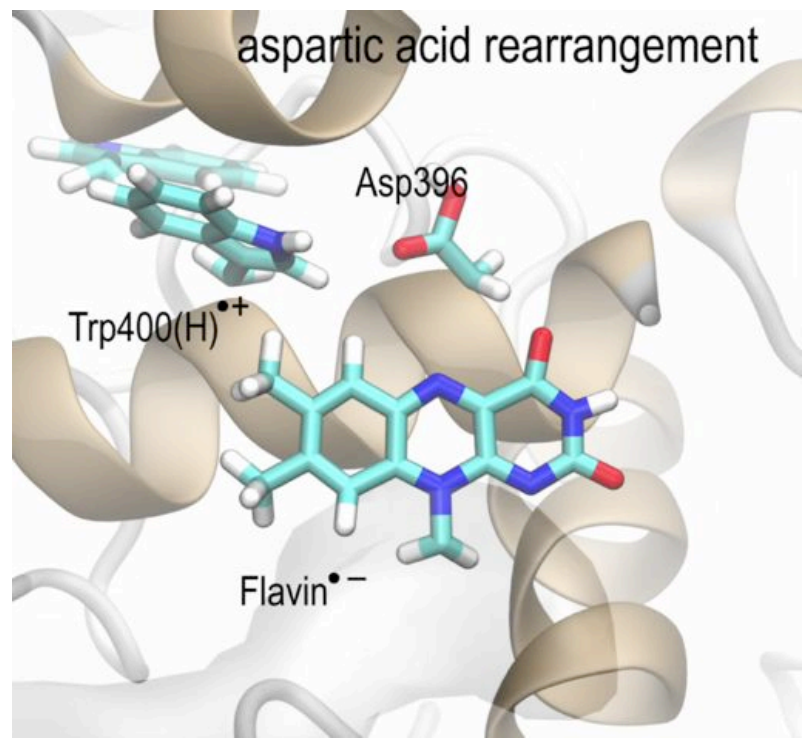

Methodology proposed: I. Solov'yov and K. Schulten, J. Phys. Chem. B (2012)

From 10,000 to 100,000 Atom MD in 2000

100k atom MD reached in 2000

- then a factor 10 increase in computation;
- **needed to describe membrane processes;**
- was achieved through cluster computing;
- produced good quality results for aquaporin;
- **is now standard.**

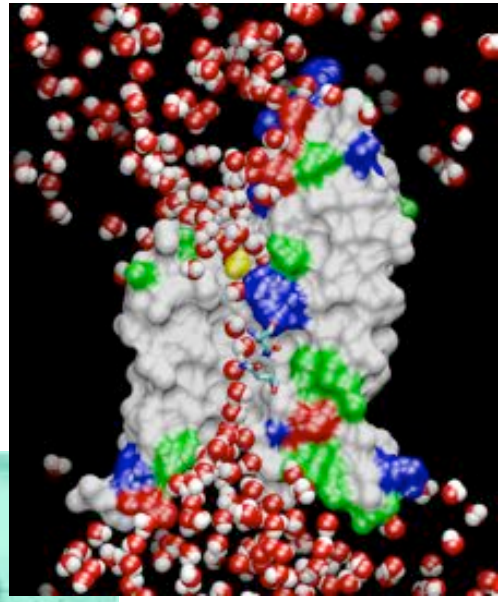

E.Tajkhorshid,
P. Nollert,
M. Jensen,
L. Miercke,
J. O'Connell,
and K. Schulten.
Science, **296:**525-530,
2002.

100,000 atoms, 12 ns

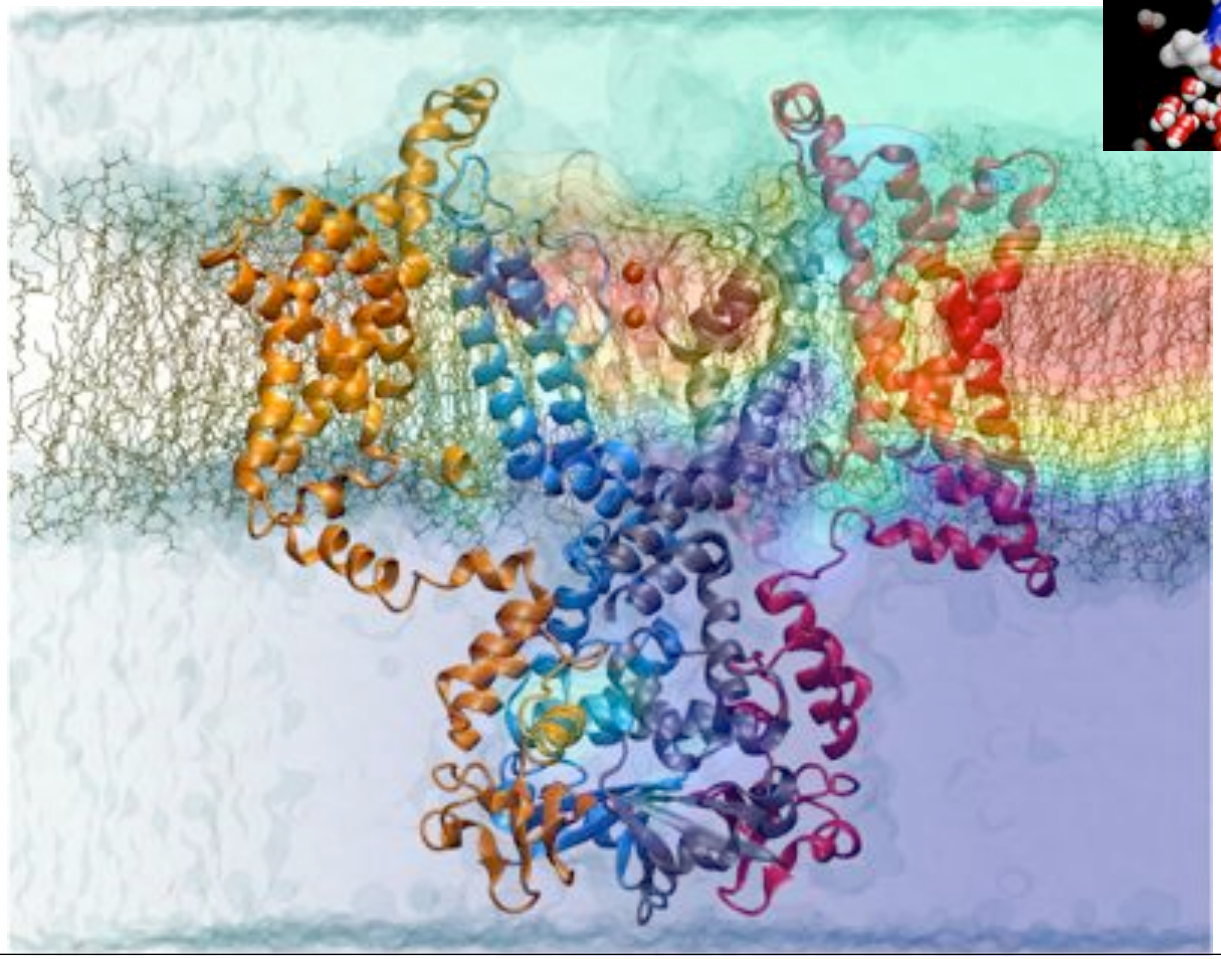

F. Khalili-Araghi, V. Jogini,
V. Yarov-Yarovoy,
E. Tajkhorshid,
B. Roux, and K. Schulten.
Calculation of the gating charge for the Kv1.2 voltage-activated potassium channel. *Biophysical Journal*, **98:**2189-2198, 2010.

350,000 atoms, 0.5 μs

From 100,000 to 20,000,000 Atom MD

100k atom MD reached in 2000

- then a factor 10 increase in computation;
- needed to describe membrane processes;
- was achieved through cluster computing;
- produced good quality results for aquaporin;
- is now standard.

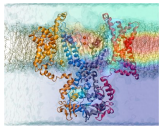

Kv1.2 voltage activated potassium channel

photosynthetic membrane of purple bacterium

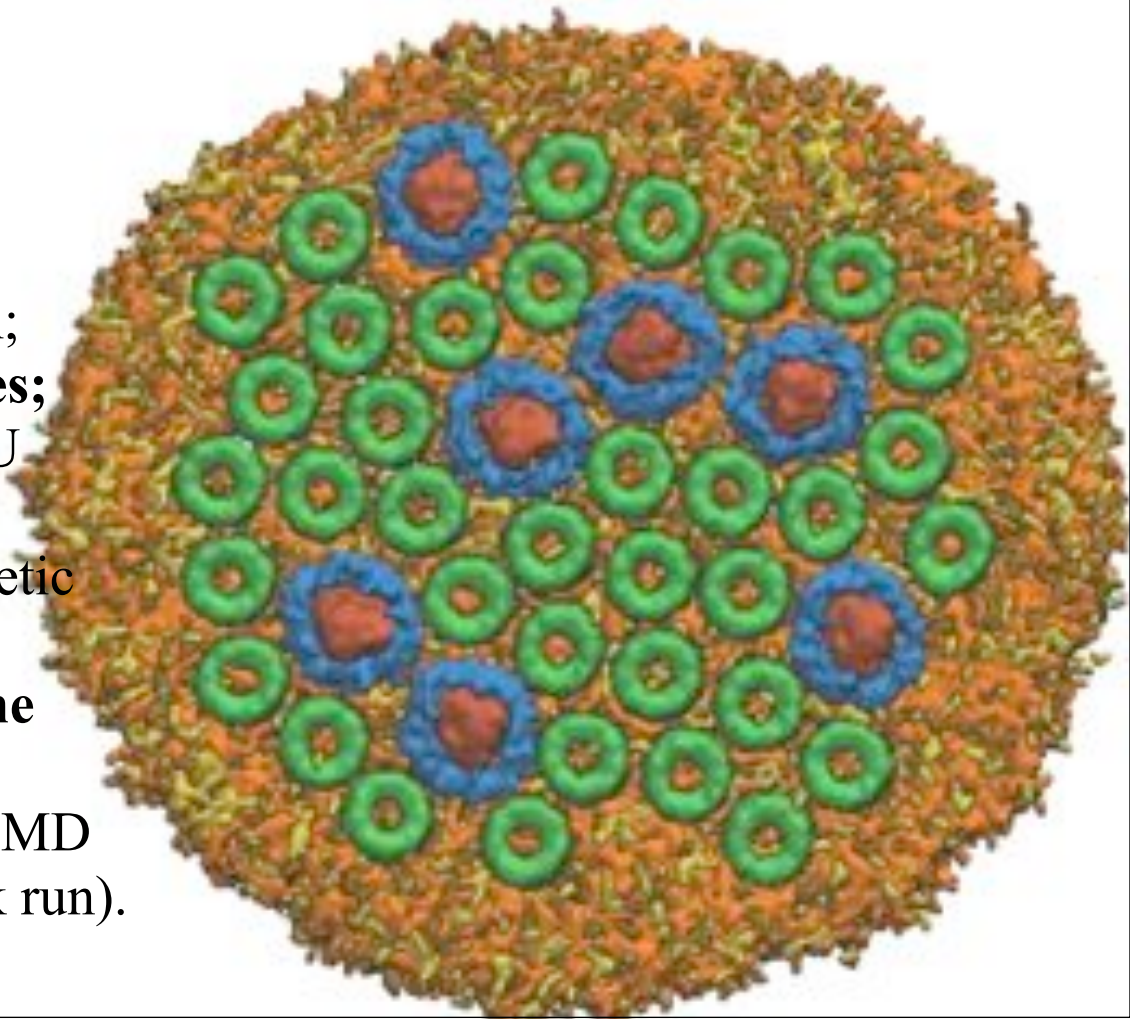

20 million atom MD reached in 2012

- a factor ~200 increase in computation;
- **needed to describe cellular processes;**
- was achieved through petascale / GPU computing;
- produced good results for photosynthetic membrane and HIV capsid;
- **will become standard as biomedicine moves to cell perspective;**
- Blue Waters makes 100 million atom MD feasible (confirmed through benchmark run).

From Electrons to Molecules to Cells

Photosynthetic Organelles in Purple Bacteria

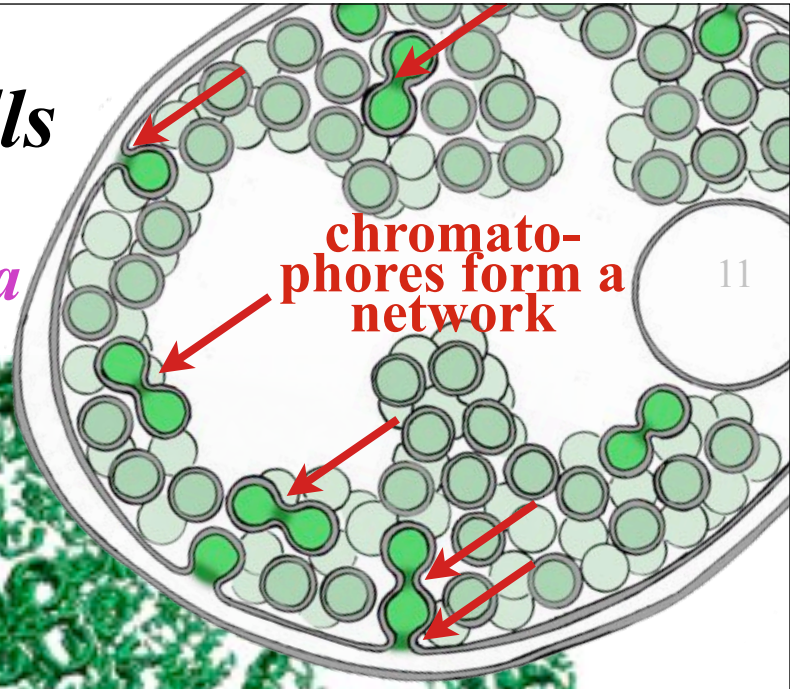

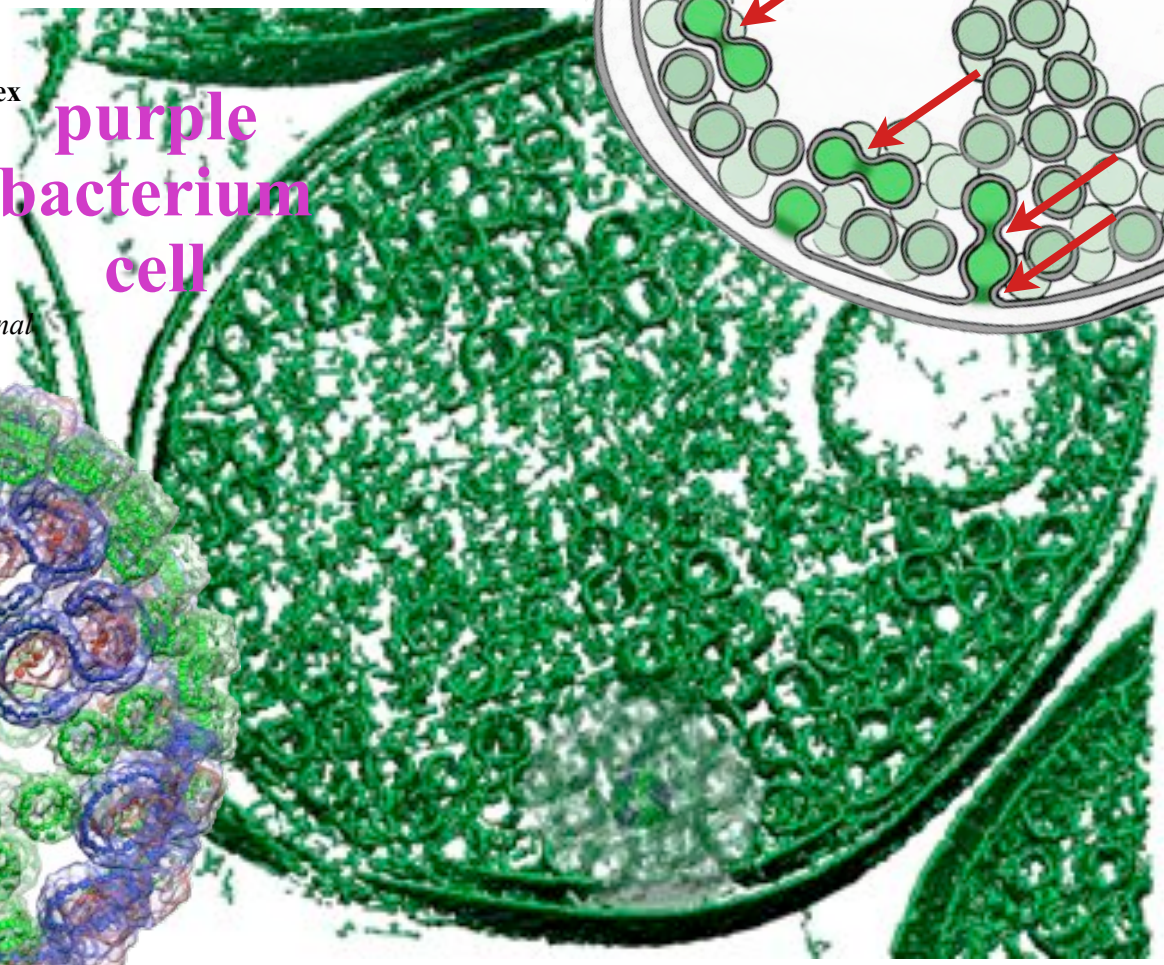

J. Strümpfer and K. Schulten. **Light harvesting complex II B850 excitation dynamics.** *Journal of Chemical Physics*, **131:**225101, 2009.

M. Sener, J. Olsen, C. Hunter, and K. Schulten. **Atomic level structural and functional model of a bacterial photosynthetic membrane vesicle.** *Proceedings National Academy of Sciences, USA*, **104**:15723-15728, 2007.

chromatophore

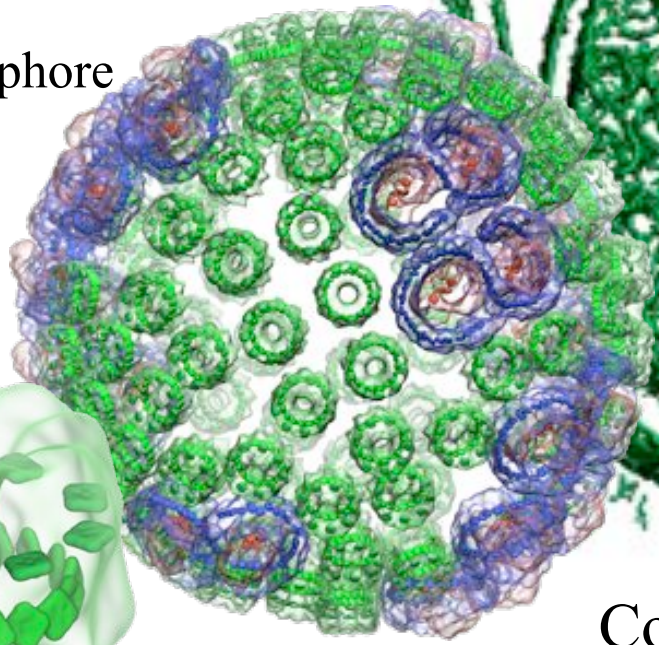

light harvesting complex 2

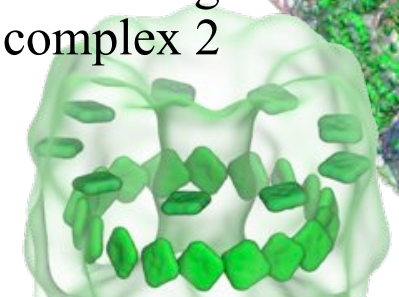

J. Koepke, X. Hu, C. Muenke, K. Schulten, and H. Michel. **The crystal structure of the light harvesting complex II (B800-850) from *Rhodospirillum molischianum*.** *Structure*, **4:**581-597, 1996.

Collaboration with **EM tomography** group of W. Baumeister, MPI Martinsried (with L. Fitting-Kourkoutis, E. Villa)

Exciton State Coherence Plays a Role in a Further Extended Excitation Energy Feeder System of LH2s (light harvesting complexes 2)

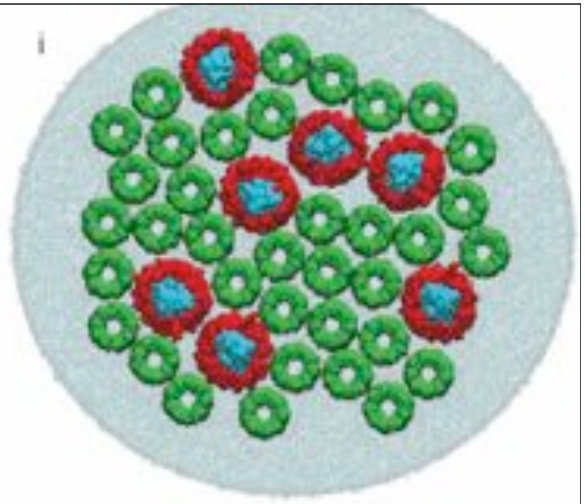

Rings of 18 Chls in LH2s form exciton bands, again with oscillator strengths coherently ‘packed” into thermally accessible states; the LH2s also add 9 Chls (with orthogonal transition dipole moments) to increase photon capture. 10 LH2s serve one LH1-RC with excitation transfer times of less than 50 ps, increasing RC “busy time” from originally (RC alone) 0.1 % to 30 %; actual numbers depend on under which light conditions bacteria grow.

Quantum coherence in the form of exciton coherence assists photosynthetic light harvesting in purple bacteria.

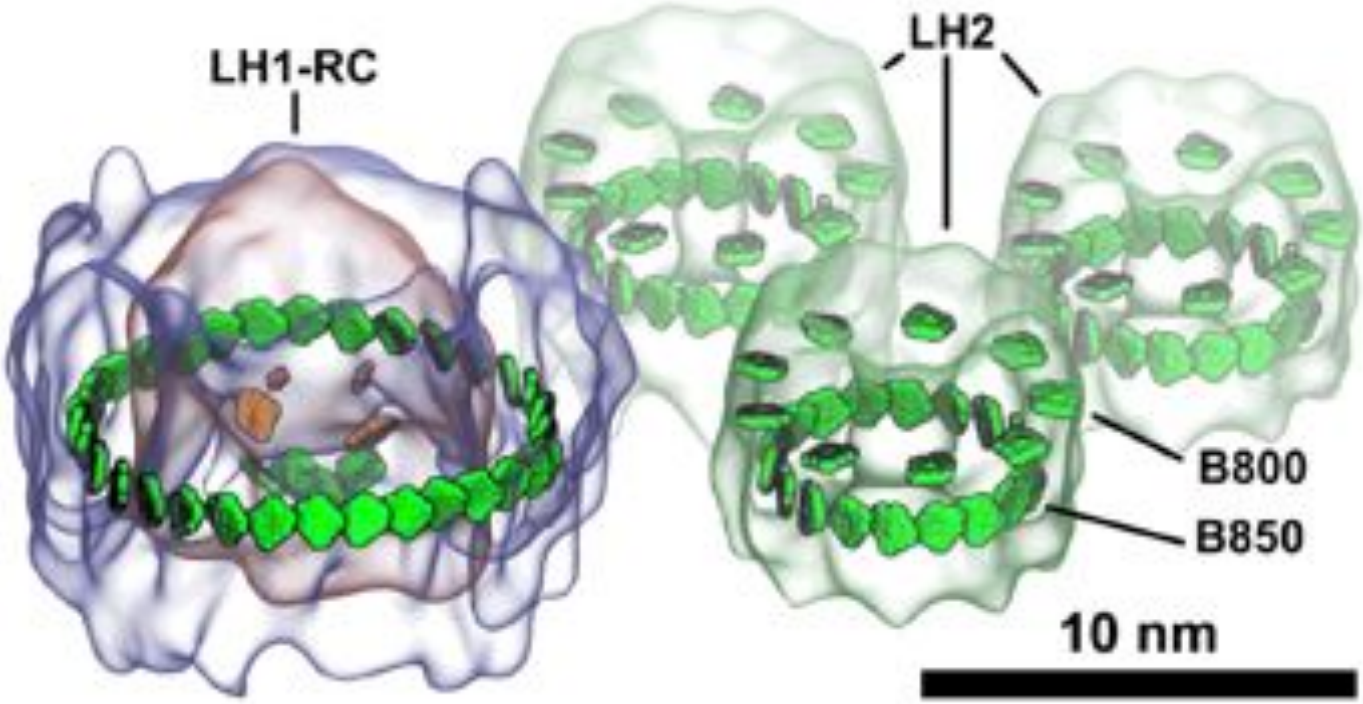

Absorption of Sun Light by Chlorophylls is Influenced by Thermal Motion

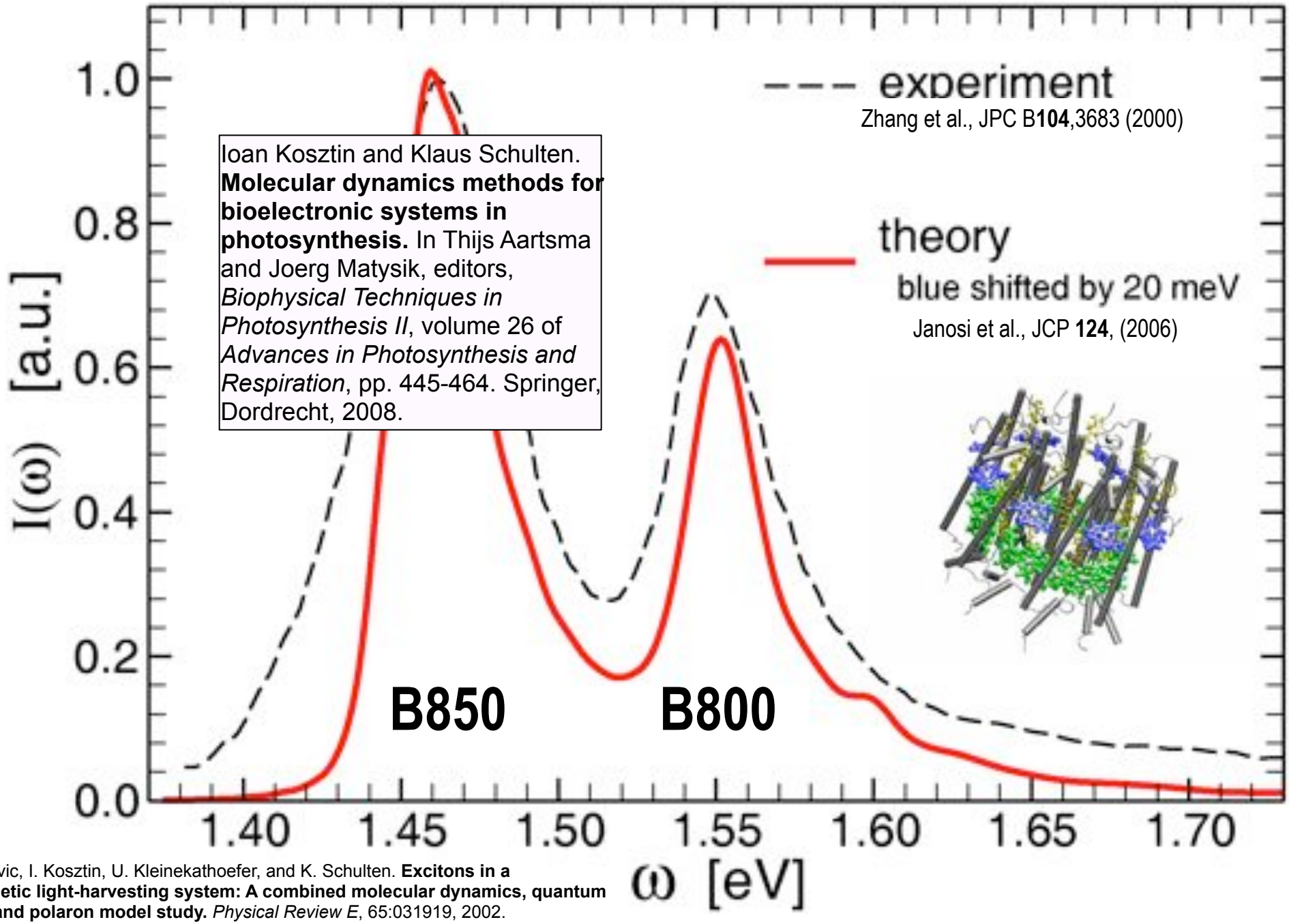

Ioan Kosztin and Klaus Schulten. **Molecular dynamics methods for bioelectronic systems in photosynthesis.** In Thijs Aartsma and Joerg Matysik, editors, *Biophysical Techniques in Photosynthesis II*, volume 26 of *Advances in Photosynthesis and Respiration*, pp. 445-464. Springer, Dordrecht, 2008.

A. Damjanovic, I. Kosztin, U. Kleinekathoefer, and K. Schulten. **Excitons in a photosynthetic light-harvesting system: A combined molecular dynamics, quantum chemistry and polaron model study.** *Physical Review E*, 65:031919, 2002.

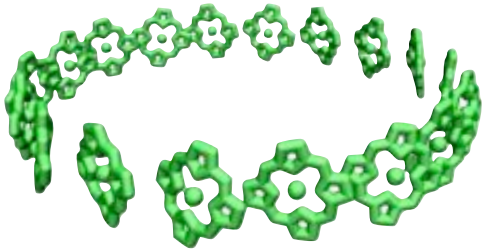

B850 Dynamics $\rho(t)$

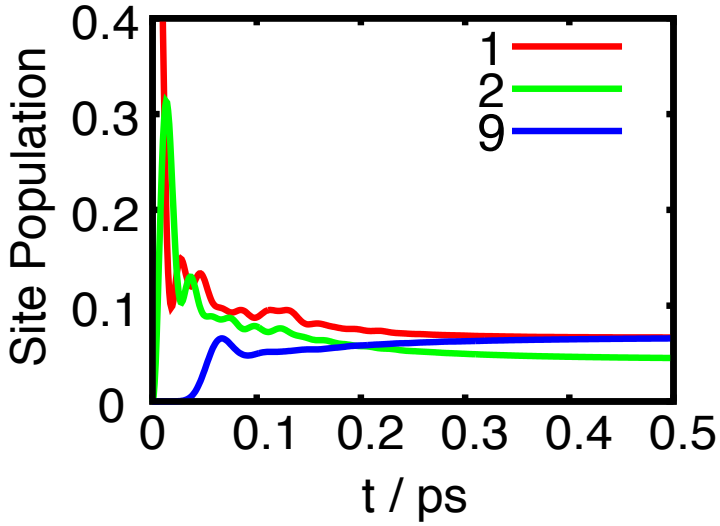

$$\rho(0) = |1\rangle\langle 1|$$

t=0.000 ps

$i = 1$

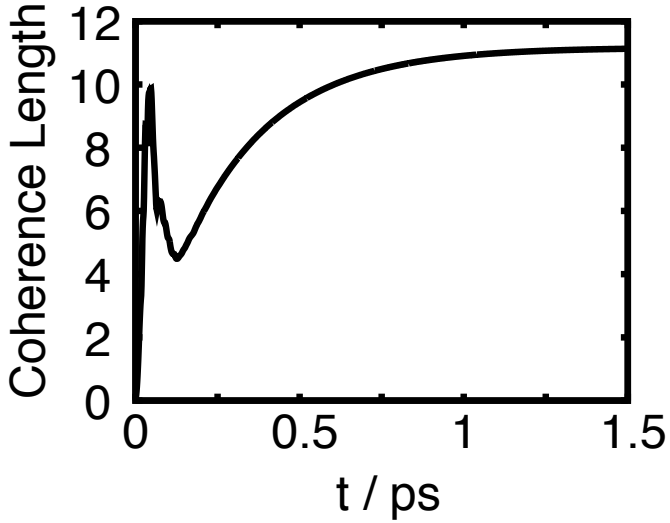

LH2 B850 at 300K

$\rho_{ii}(t)$ $\rho_{ij}(t)$ $i \neq j$

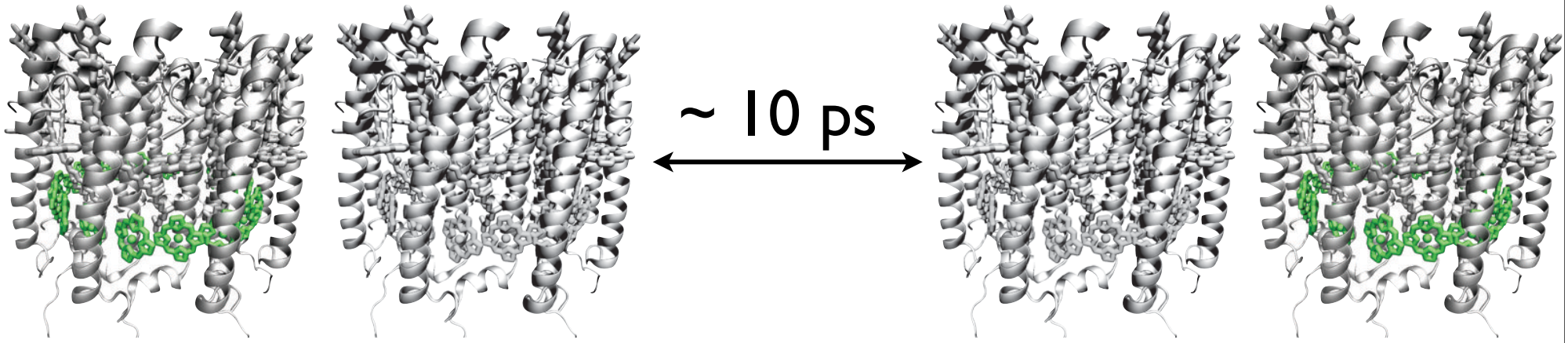

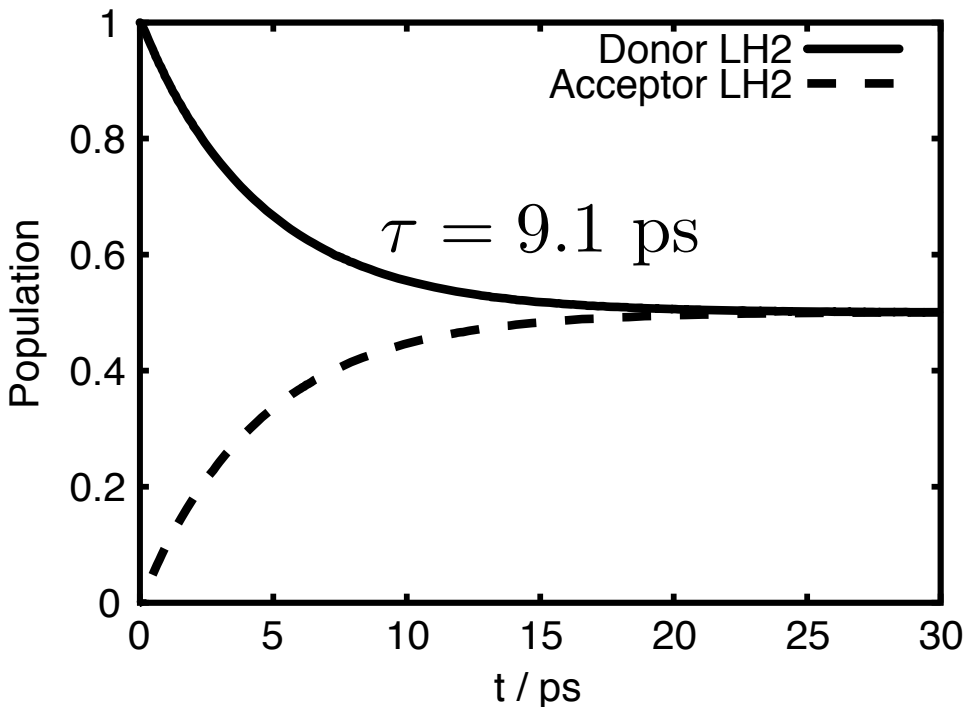

Single exponential fit
=> Incoherent transfer

- Generalised Förster: 10.2 ps (0.23 secs, 1 cpu)
- HEOM calculation: 9.1 ps (20.8 days, 16 cpus)

J. Strümpfer and K. Schulten. **Light harvesting complex II B850 excitation dynamics.** *J. Chemical Physics*, 131:225101, 2009; J.Strümpfer and K. Schulten. **The effect of correlated bath fluctuations on exciton transfer.** *J. Chemical Physics*, 134:095102, 2011.

$$\mathcal{T}_{DA} = \frac{2\pi}{\hbar} \sum_{m\in D} \sum_{n\in A} \frac{e^{-E_m^D/k_BT}}{\sum_{l\in D} e^{-E_l^D/k_BT}} \left|V_{mn}^{DA}\right|^2 \int dE\, S_m^D(E) S_n^A(E)$$

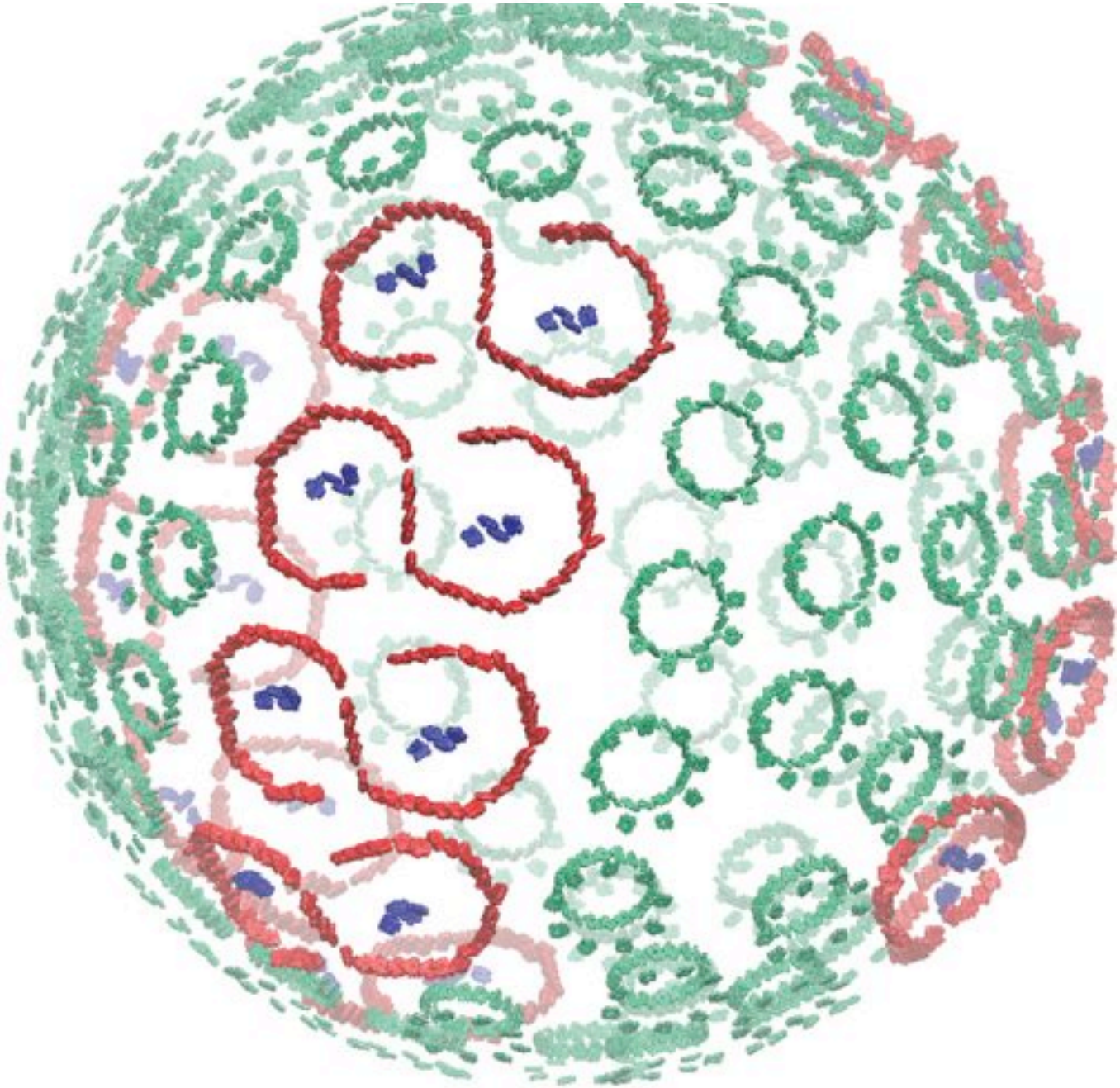

Excitation transfer through fluorescent resonant energy transfer (FRET) in photosynthetic light harvesting

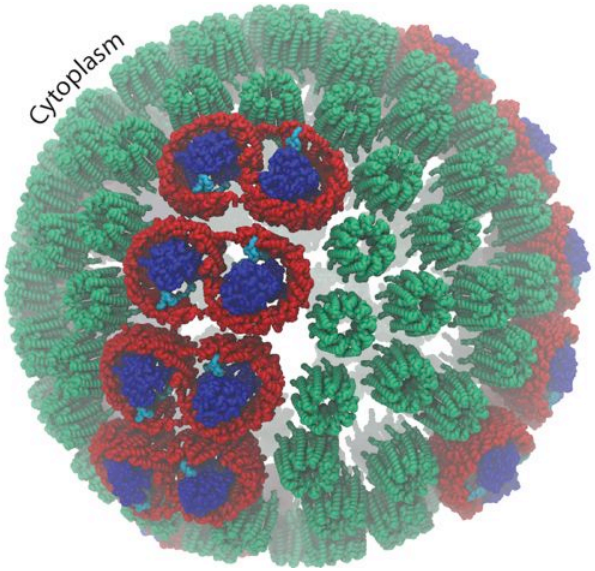

Molecular Dynamics Flexible Fitting (MDFF) Method

Electron microscopy

FEI microscope

MDFF

X-ray crystallography

APS at Argonne

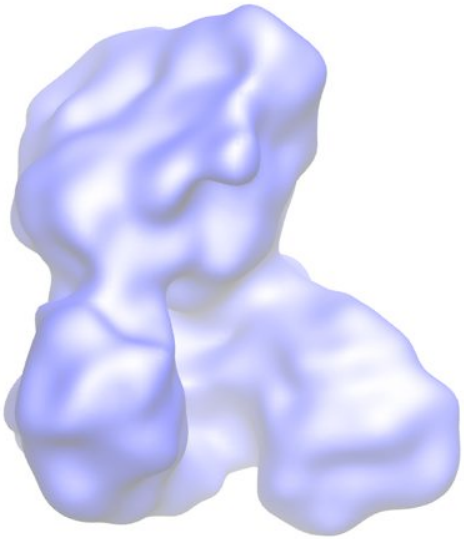

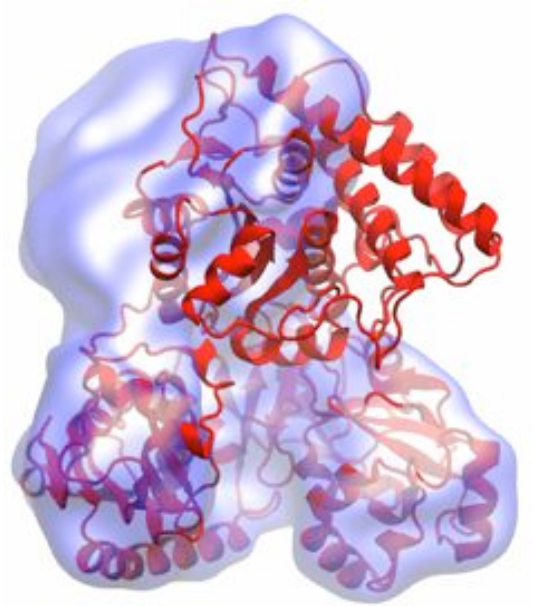

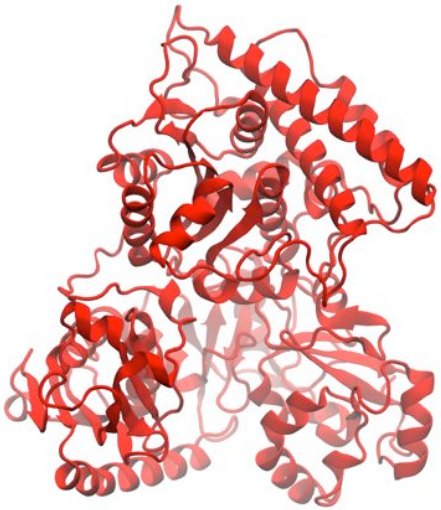

Acetyl – CoA Synthase

L. Trabuco, E. Villa, K. Mitra, J. Frank, and K. Schulten. Flexible fitting of atomic structures into electron microscopy maps using molecular dynamics. Structure, 16:673-683, 2008.

BTRC Joins Computation and Experiment in Virology

Molecular Dynamics Flexible Fitting of Tubular HIV Capsid:

In the tubular geometry the capsid contains only hexameric subunits.

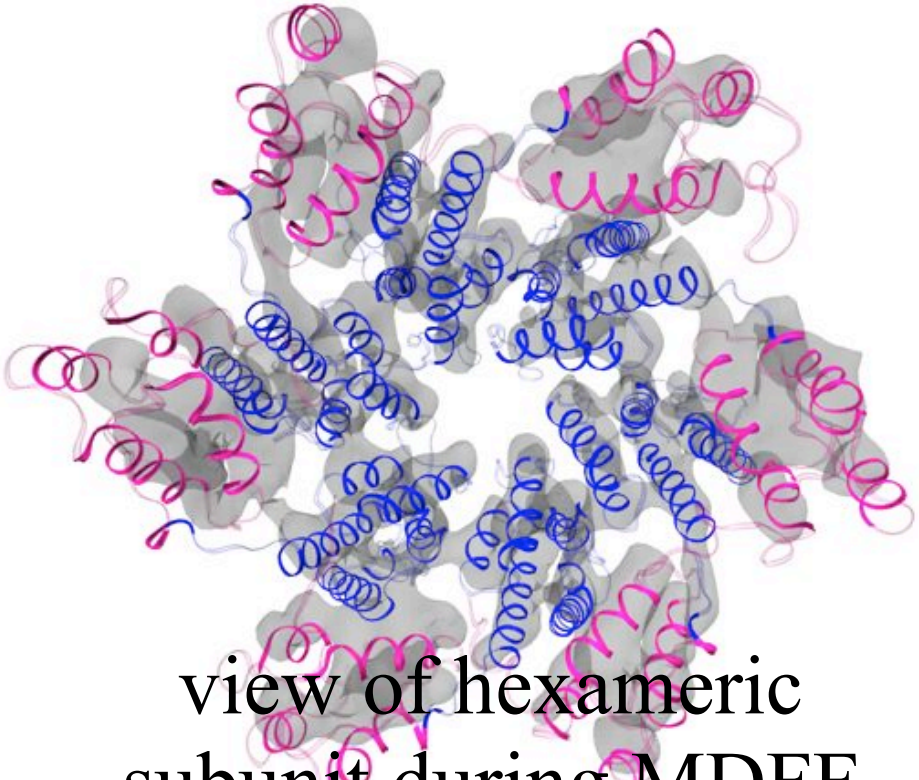

view of hexameric subunit during MDFF

final cross-correlation 0.96

Relaxation of capsid segment requires 13 million atom MD simulation on Blue Waters, 50 ns ns done

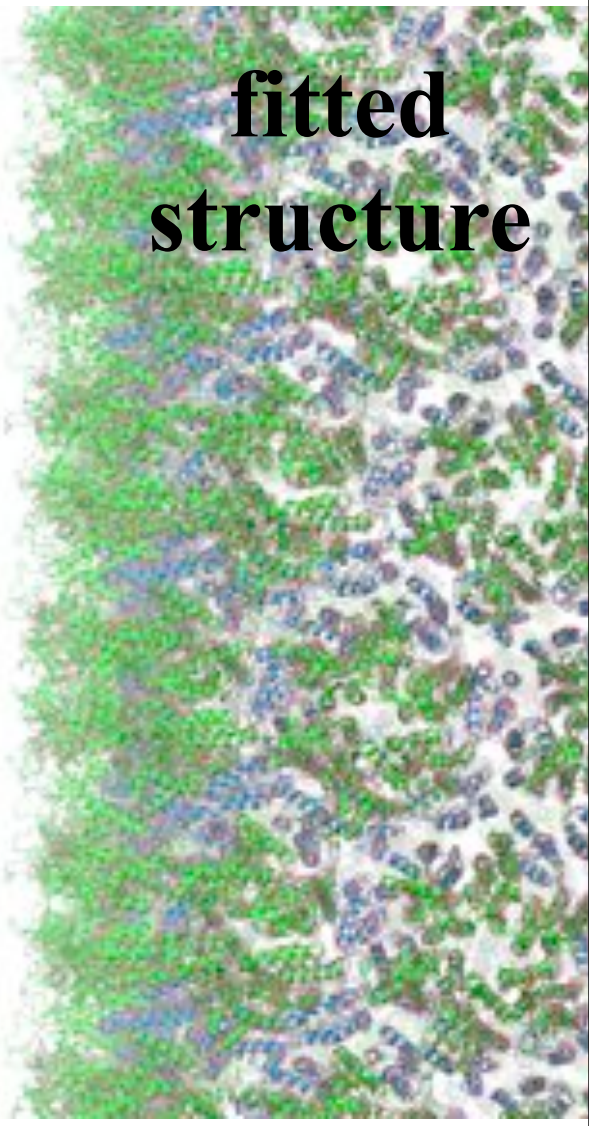

Recent MDFF application: Intra-ring cooperation in group II chaperonins

Collaboration with Fei Sun (Chinese Academy of Sciences)

Zhang et al. Submitted. Mar 2012

Symmetry-restrained MDFF applied to 12 EM maps revealed role of electrostatic interaction in chaperonin hetero-oligomer formation

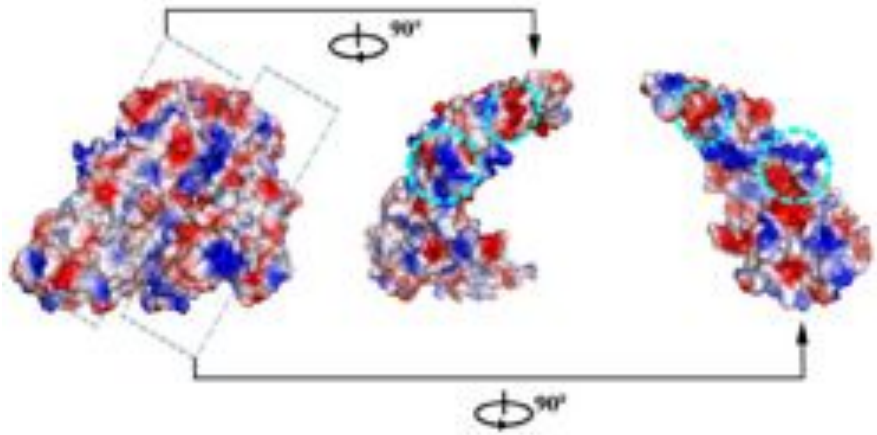

EM Maps of Various Chaperonin Conformations

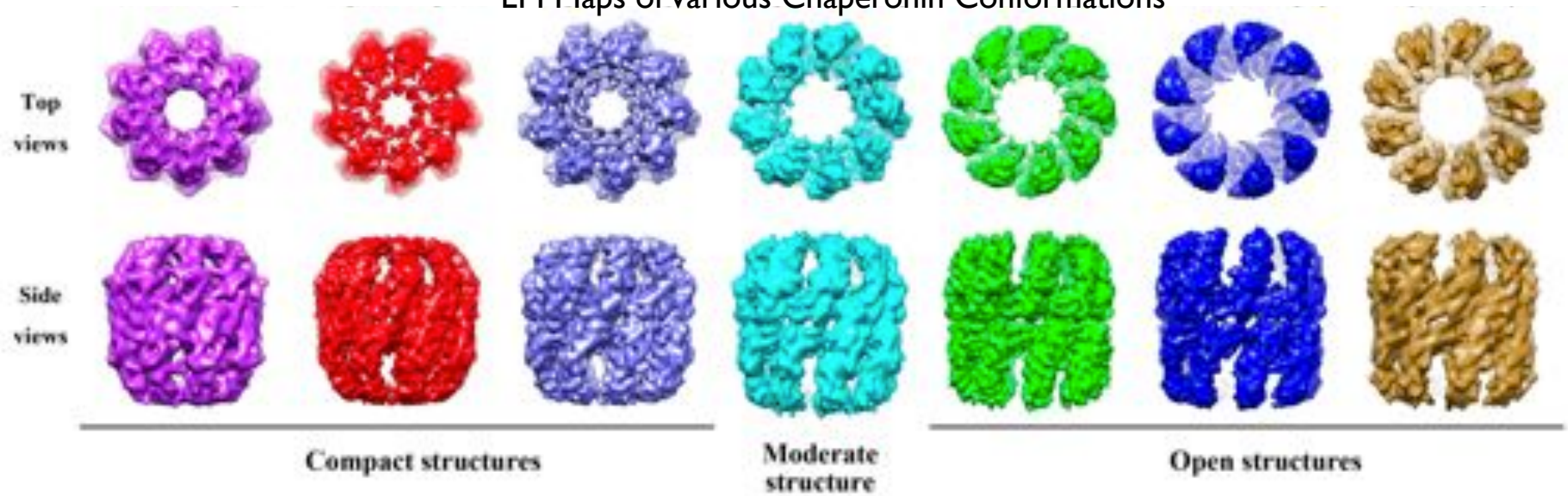

MDFF is young (2008), yet already successful

Over 30 reports of MDFF applications:

- ***By Group Researchers:***

  Villa et al. ***PNAS*** (2009): EF-Tu ribosome complex
  Seidelt et al. ***Science*** (2009): TnaC ribosome translation stalling
  Becker et al. ***Science*** (2009): Sec61 ribosome complex
  Frauenfeld et al. ***Nat. Struct. Mol. Biol***. (2011): SecYE ribosome complex
  Agirrezabala et al. ***PNAS*** (2012): Ribosome translocation intermediates
  Zhang et al. Submitted. Mar 2012: Chaperonins

- ***By Outside Researchers:***

  Lorenz et al. ***PNAS*** (2010): actin-myosin interface
  Bhushan et al. ***Nat. Struct. Mol. Biol***. (2010): α-helical nascent chains
  Armache et al. ***PNAS*** (2011): Eukaryotic ribosomal proteins
  Armache et al. ***PNAS*** (2011): Translating eukaryotic ribosome
  Guo et al. ***PNAS*** (2011): RsgA GTPase on ribosomal subunit
  Becker et al. ***Nat. Struct. Mol. Biol***. (2011) Dom34–Hbs1 stalled ribosome complex
  Wollmann et al. ***Nature*** (2011): Mot1–TBP complex
  Strunk et al. ***Science*** (2011): Ribosome assembly factors
  Lasker et al. ***PNAS*** (2012): Proteasome
  Becker et al. ***Nature*** (2012): Ribosome recycling complex

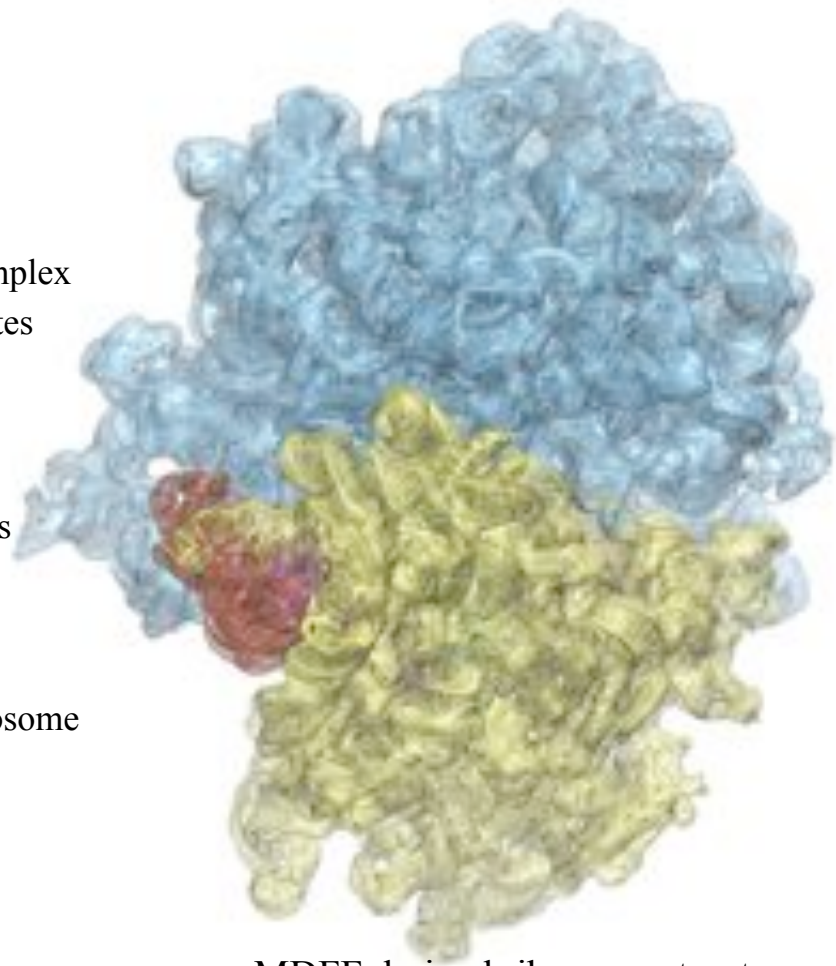

MDFF derived ribosome structure
Villa et al. *PNAS* 2009

Tightly integrated into NAMD and VMD

- Capable of quickly fitting very large structures
- Adaptable to a wide range of applications

Science 3: How Proteins AreMade from Genetic Blueprint

Low-resolution data

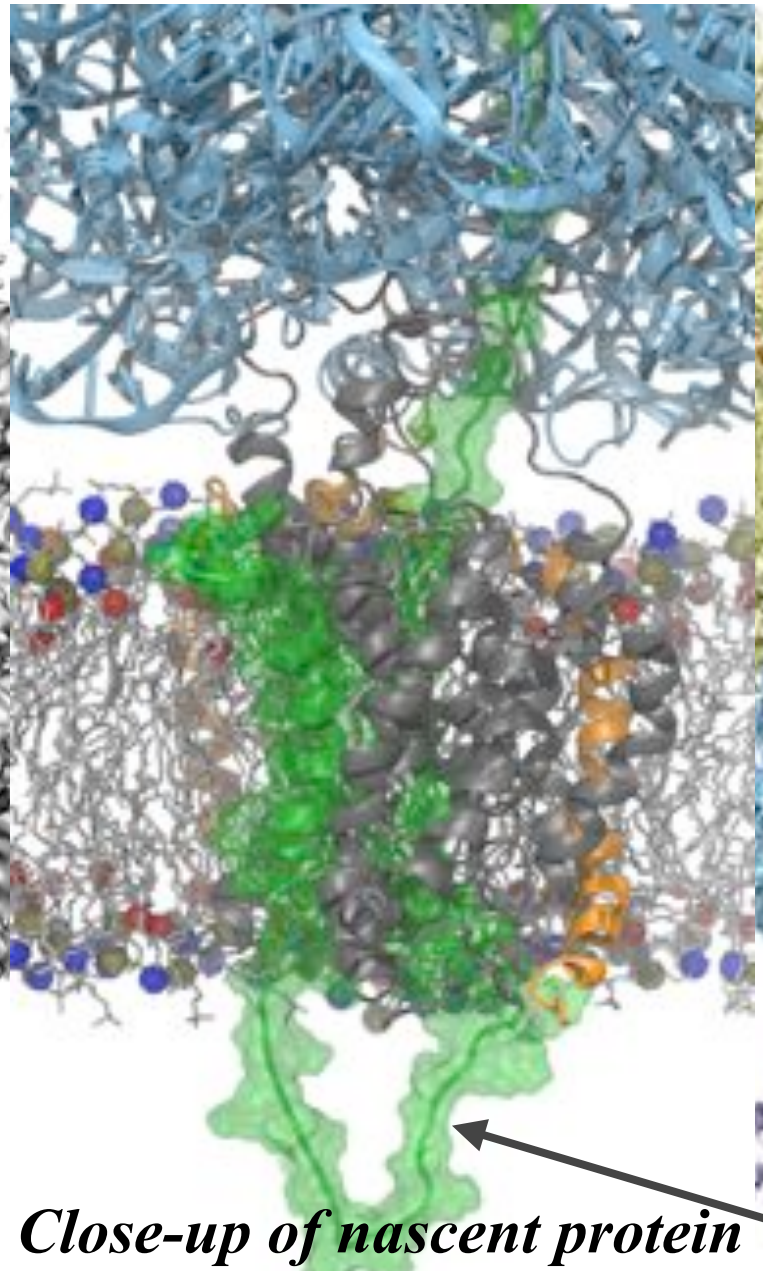

High-resolution structure

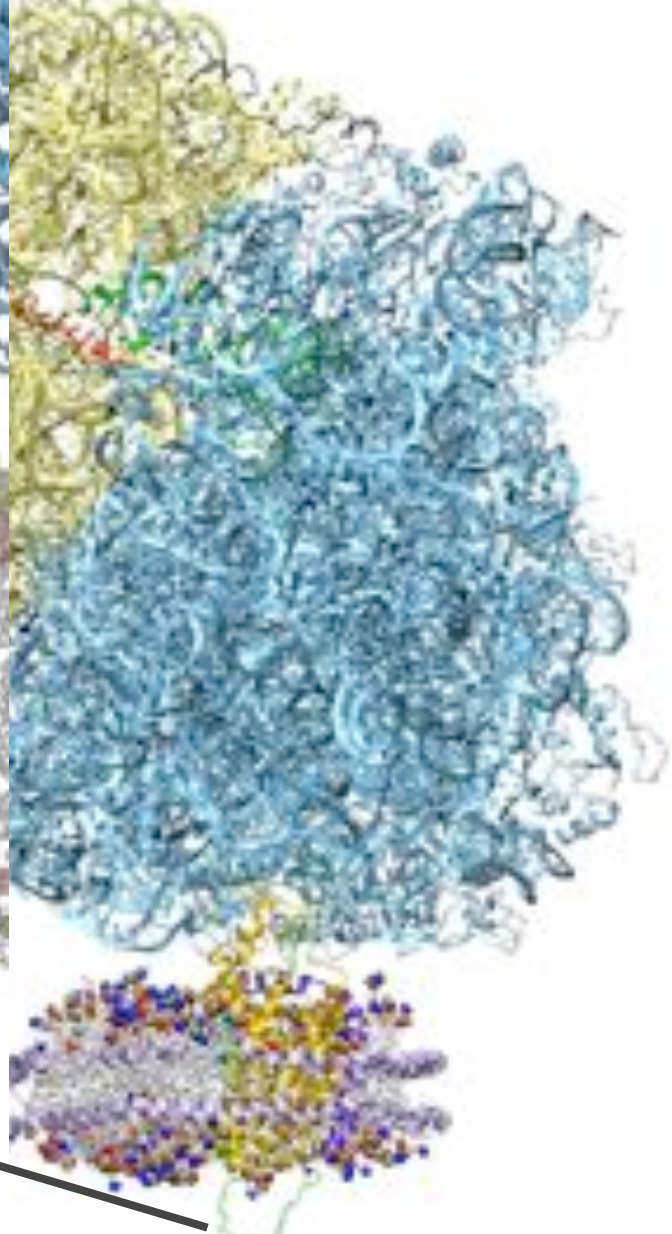

Close-up of nascent protein

Frauenfeld, Gumbart et al. *Nat. Struct. Mol. Bio.* **18**, 614-621, 2011.

Molecular Dynamics Flexible Fitting (MDFF) Study of the Localization of Nascent Proteins

Ribosome expressing membrane protein

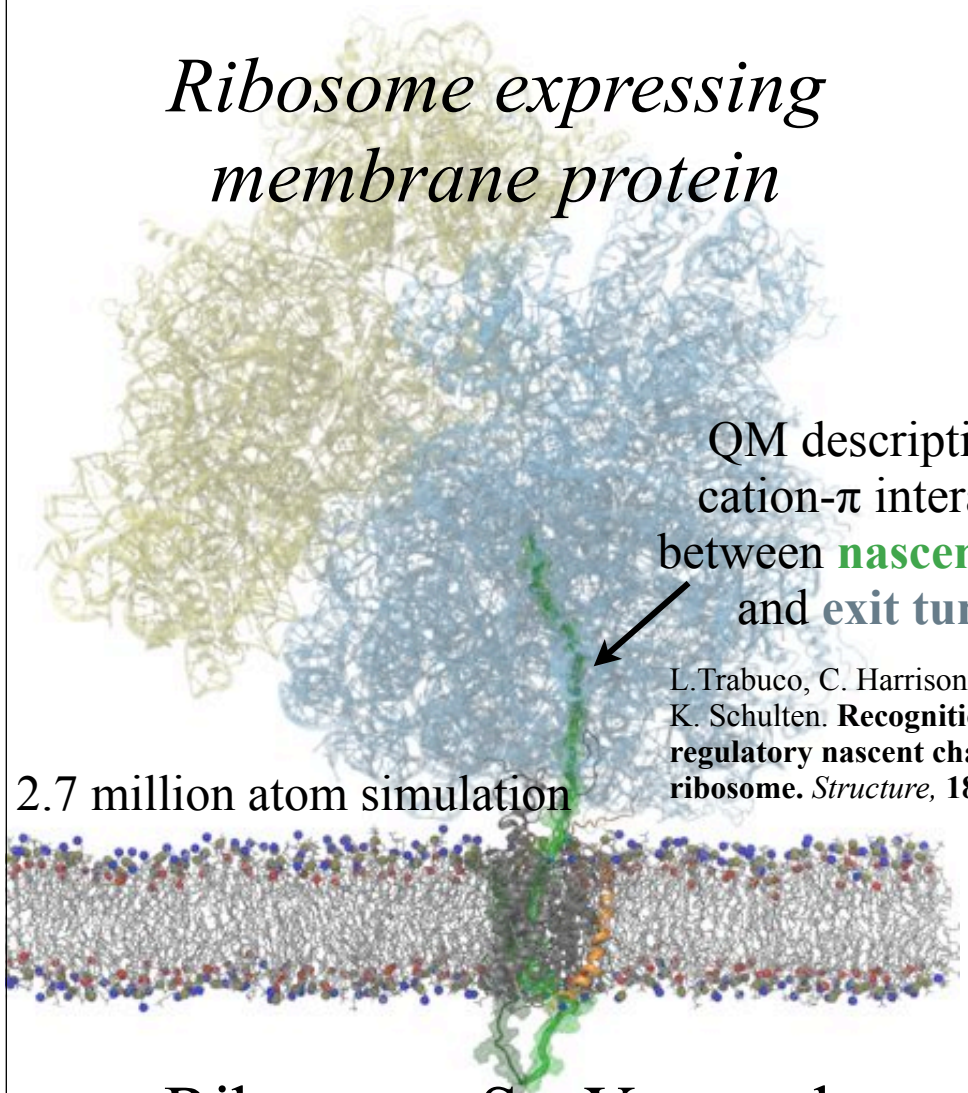

QM description of cation-π interaction between **nascent chain** and **exit tunnel**

L.Trabuco, C. Harrison, E. Schreiner, and K. Schulten. **Recognition of the regulatory nascent chain TnaC by the ribosome.** *Structure,* **18:**627-637, 2010.

2.7 million atom simulation

Ribosome-SecY-complex

Ribosome expressing a cytosolic protein

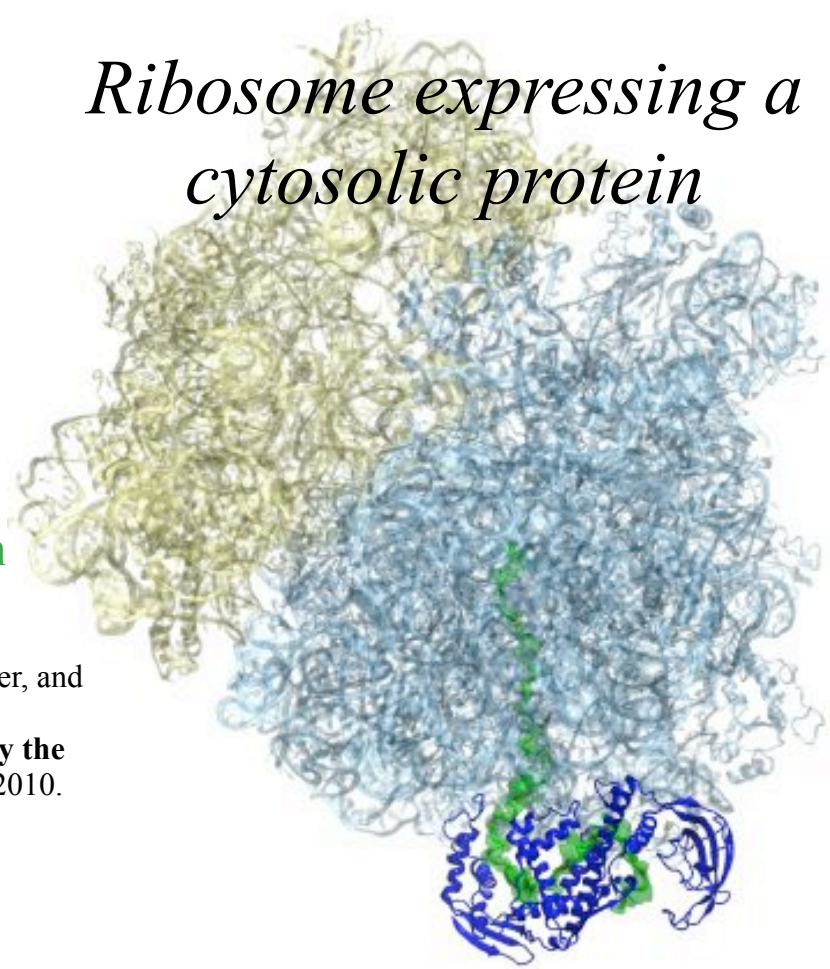

Ribosome-Trigger Factor-complex

Frauenfeld, Gumbart et al. *Nat. Struct. Mol. Bio.* **18**, 614-621, 2011.

Structural characterization of mRNA-tRNA translocation intermediates

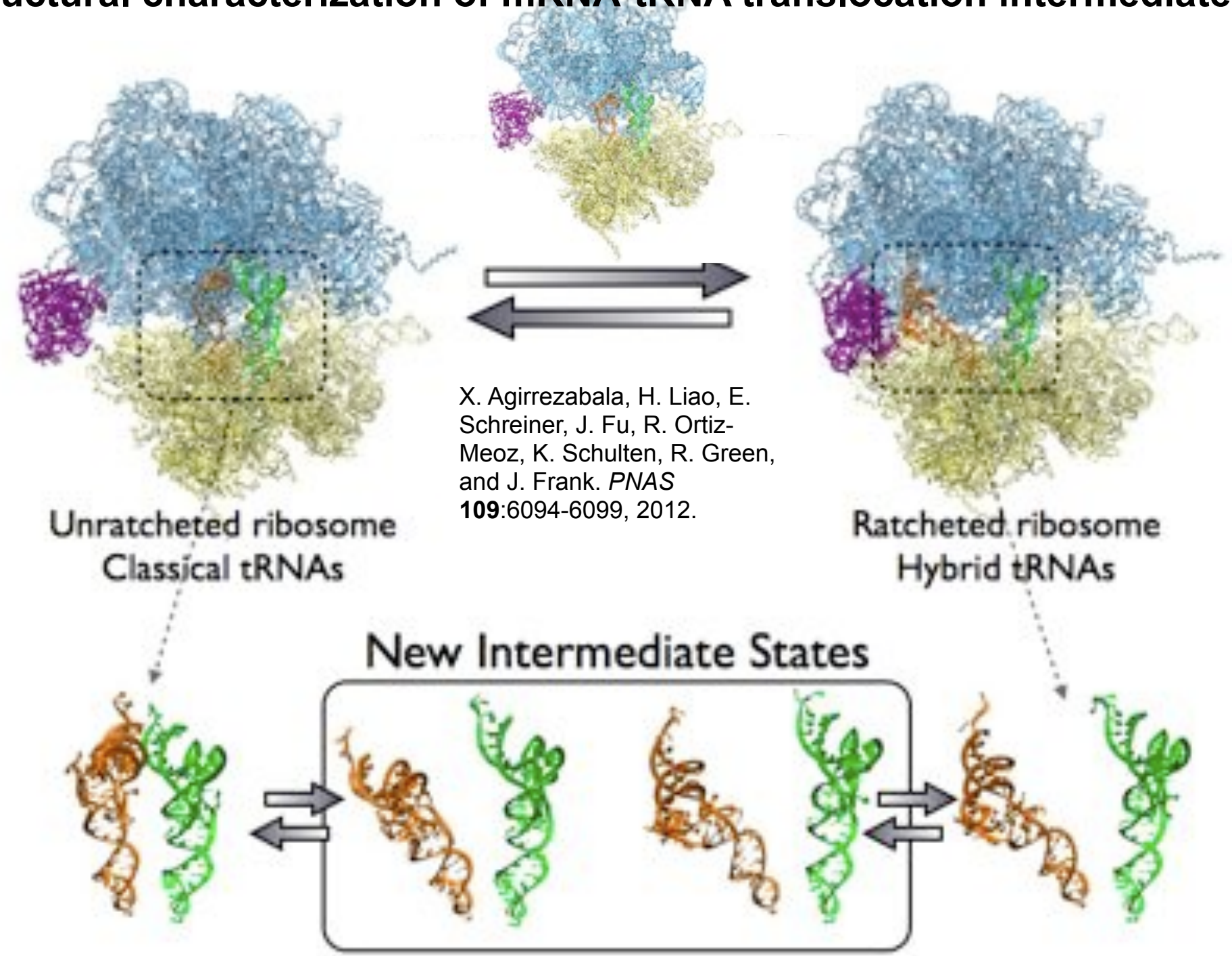

X. Agirrezabala, H. Liao, E. Schreiner, J. Fu, R. Ortiz-Meoz, K. Schulten, R. Green, and J. Frank. *PNAS* **109**:6094-6099, 2012.

Design of Tyrosine Kinase Sensor

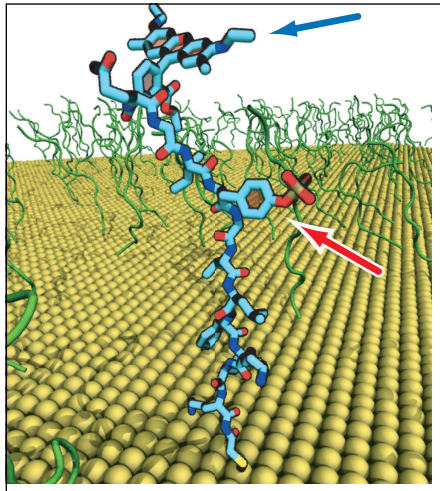

- Peptides are attached to a gold surface. The end of oligopeptide contains rhodamine.
- Peptides are exposed to ATP and appropriate kinase.
- Electric field is applied; change in conformation depends on phosphorylation state.
- Distance from rhodamine determines magnitude of fluorescence signal.

initial sequence: {1 GLU} {2 GLY} {3 ILE} {4 TYR} {5 GLY} {6 VAL} {7 LEU} {8 PHE} {9 LYS} {10 LYS} {11 LYS} {12 CYS}

Rhodamine (R6g)

Tyrosine residue interacts with kinases by phosphorylation

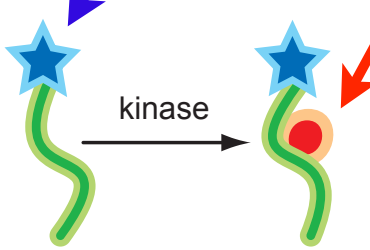

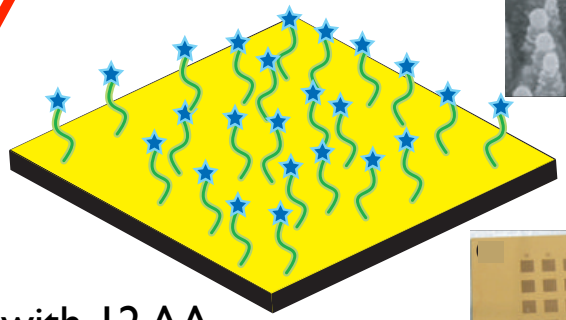

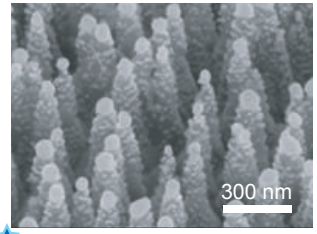

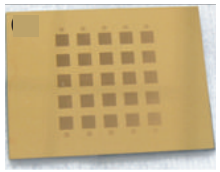

Au surface, oligopeptide with 12 AA, bound via sulfide bond

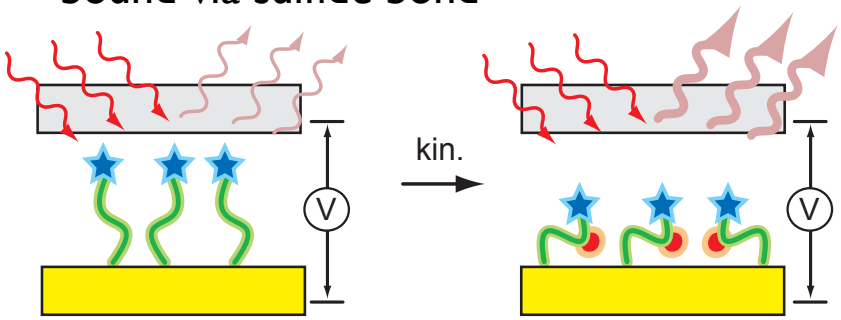

Experiment: Logan Liu and Yi Chen, Nano Lab, U. Illinois

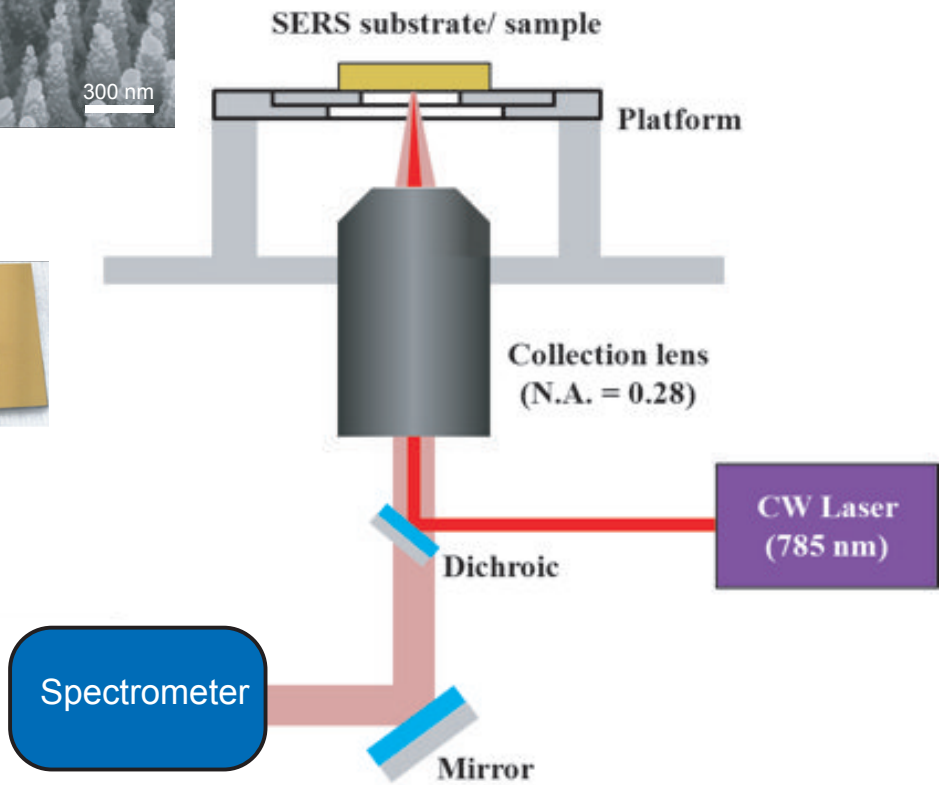

MD Simulations Revealed Problems in Design

initial sequence: {1 GLU} {2 GLY} {3 ILE} {4 TYR} {5 GLY} {6 VAL} {7 LEU} {8 PHE} {9 LYS} {10 LYS} {11 LYS} {12 CYS}

Initial sequence did not work due to surface adhesion and rhodamine aggregation

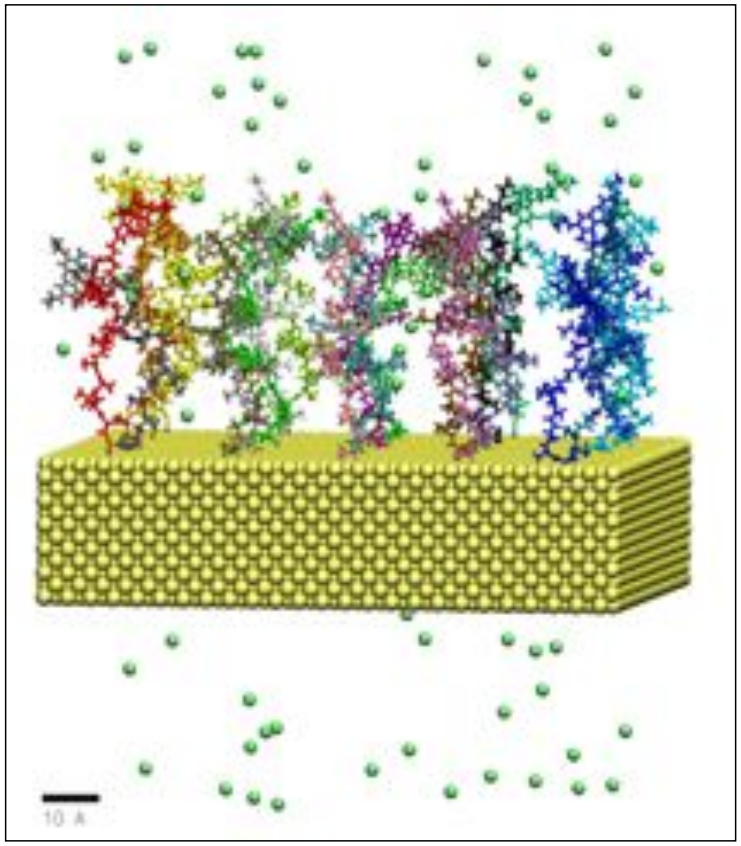

- MD systems include gold surface, water, ions and 5x5 peptide grid, ~ 100,000 atoms.
- Different sequences tested under positive and negative volt biases.

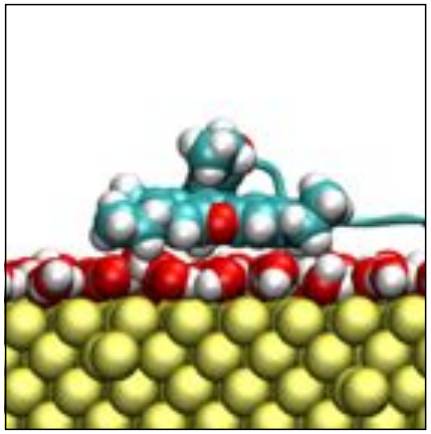

- **Improved sequence**. Avoid residues that strongly bind to gold surface.

- **Rhodamines molecules tend to aggregate**.

Aggregation affects peptide bending.

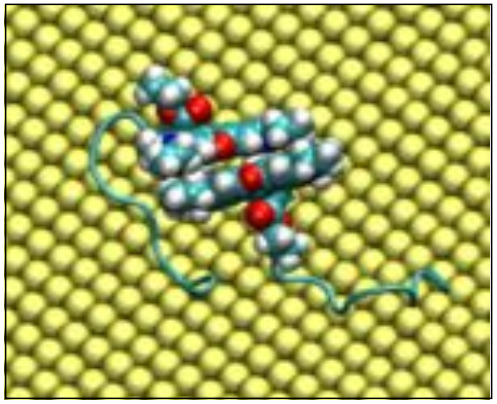

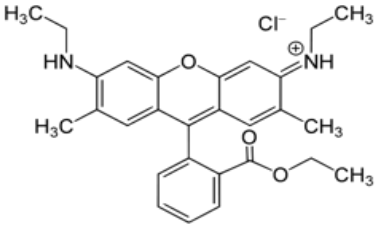

Current Design Improved

New sequence: rhodamin removed and measurement replaced by Raman spectroscopy

Rhodamine removed,
Fluorescence signal discarded

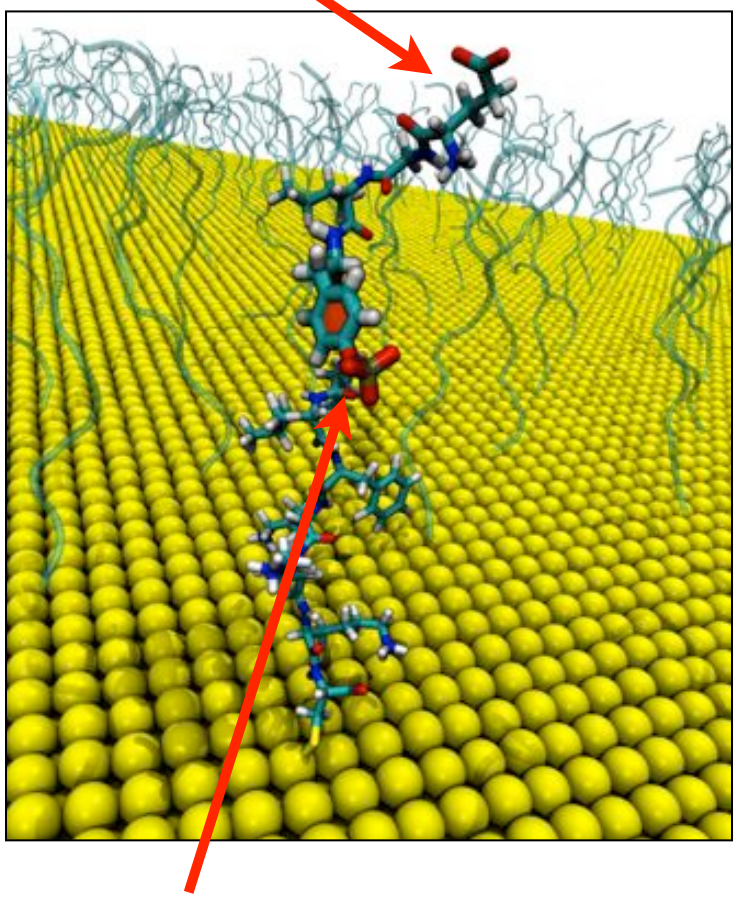

Phosphorylated tyrosine

MD Simulations show that phosphorylated tyrosine bends the peptide depending on voltage polarity

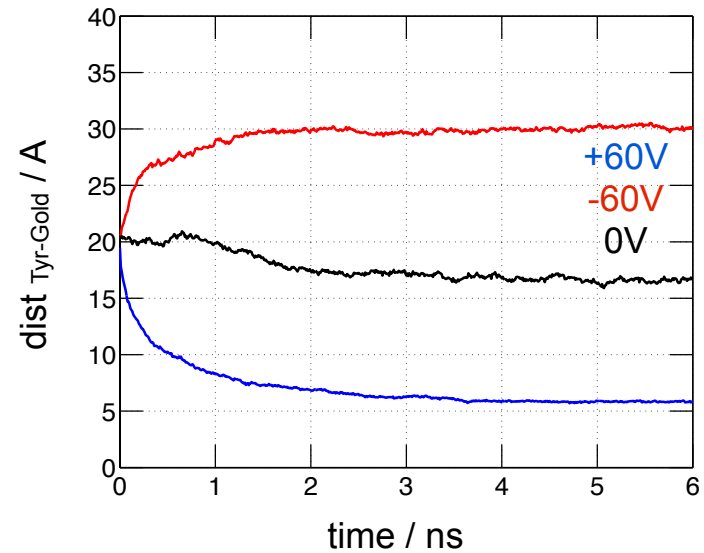

Experiments show that peptide bends towards the surface at positive voltages, increasing the intensity of Raman shifts.

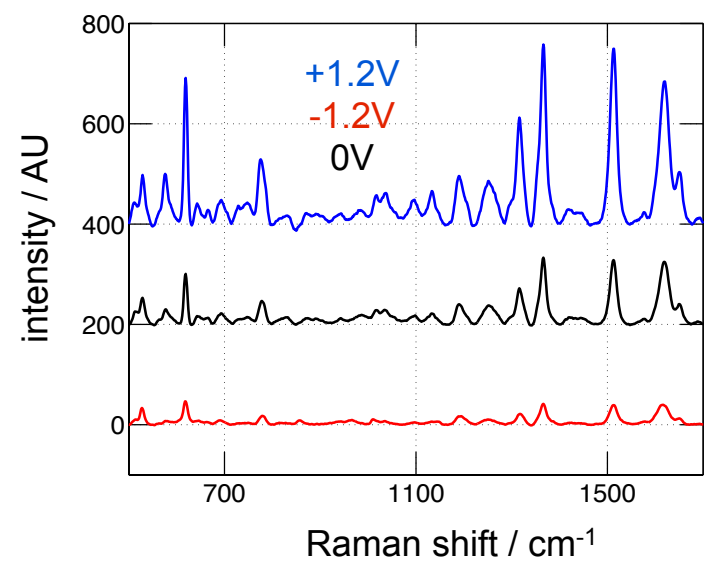

Peptide bending is now measured with Raman Spectroscopy.
The detection relies on careful comparison of peak points

Unphosphorylated

EGI**Y**GVLFKKKC-*AU*

Phosphorylated

EGI(**pY**)GVLFKKKC-*AU*

Simulation

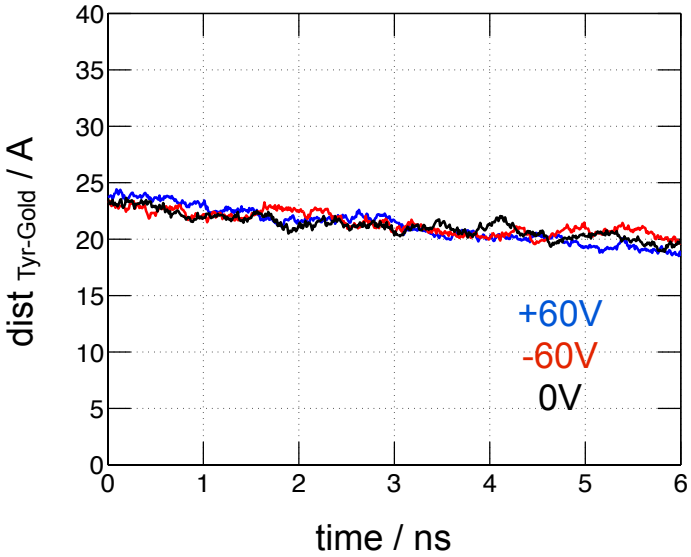

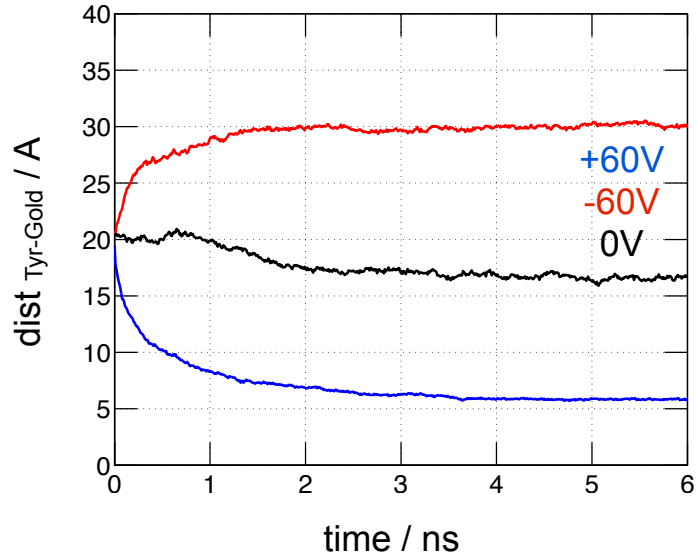

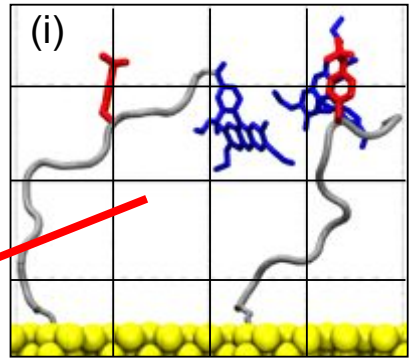

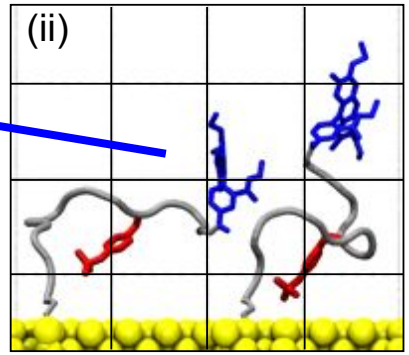

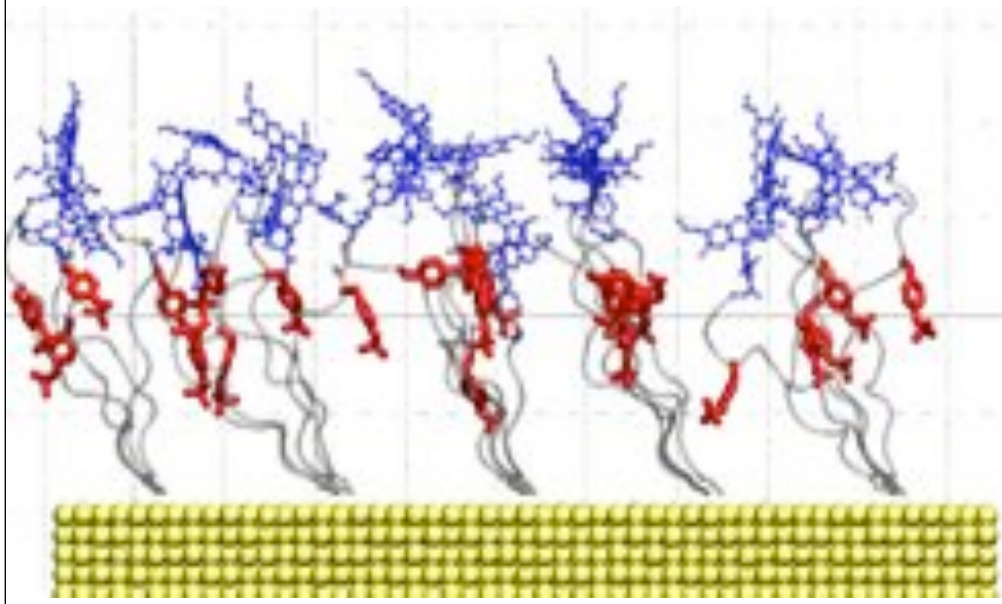

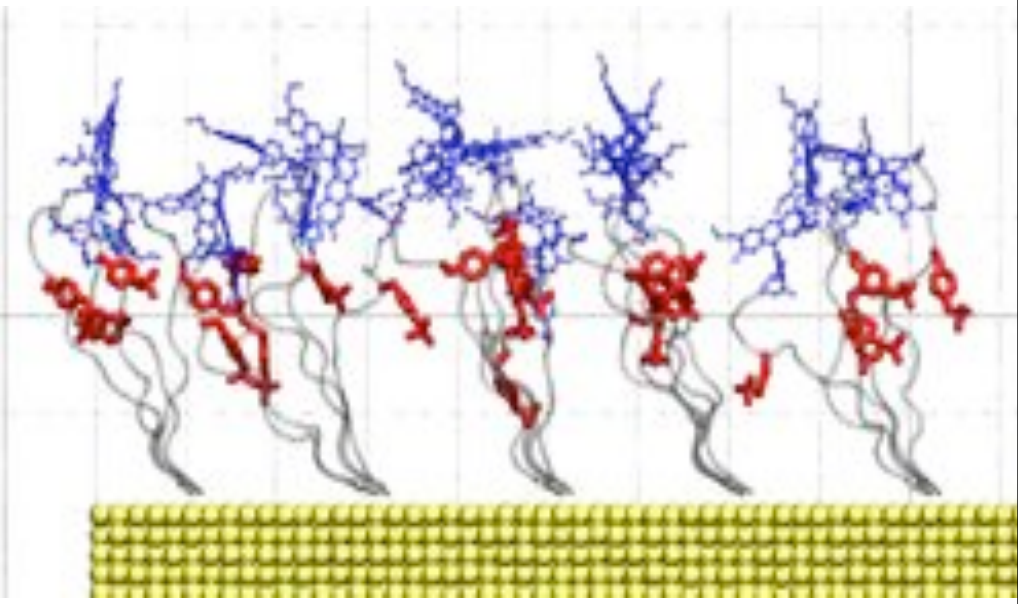

Unphosphorylated

EGI**Y**GVLFKKKC-*AU*

Phosphorylated

EGI(**pY**)GVLFKKKC-*AU*

Simulation

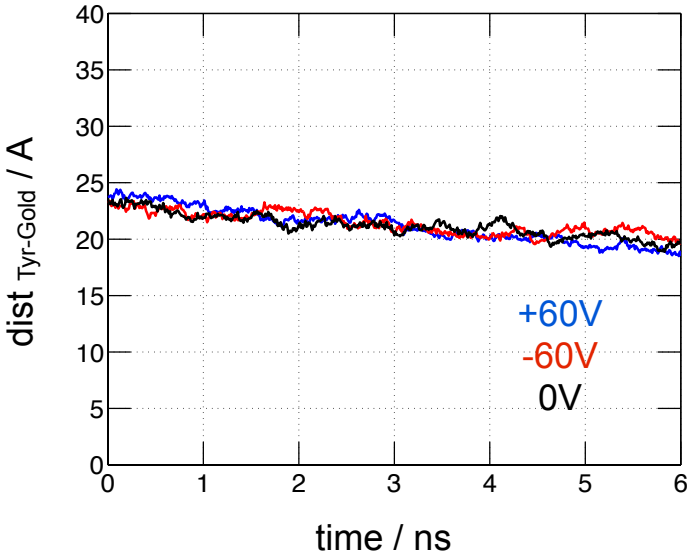

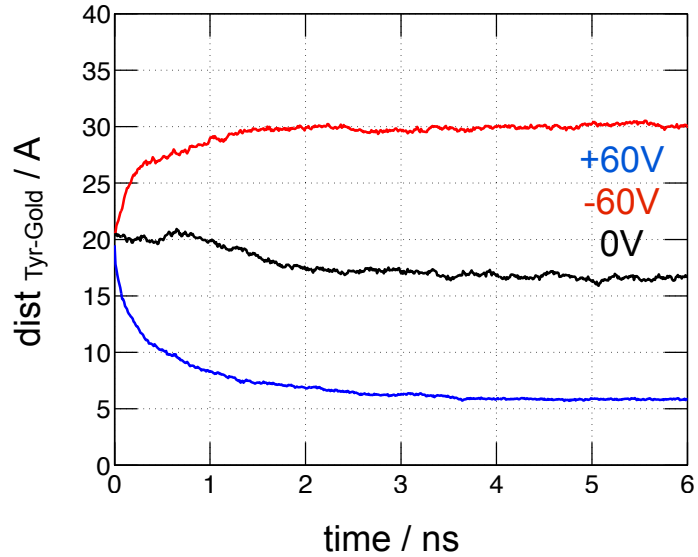

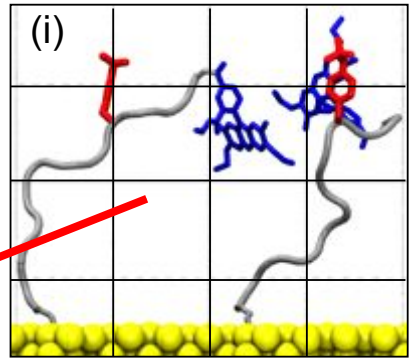

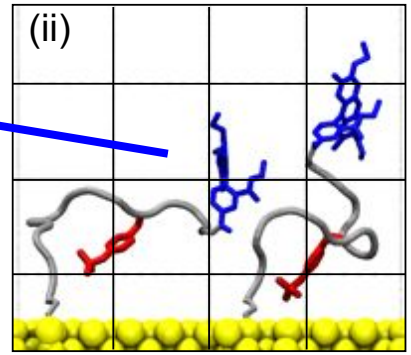

Experiment

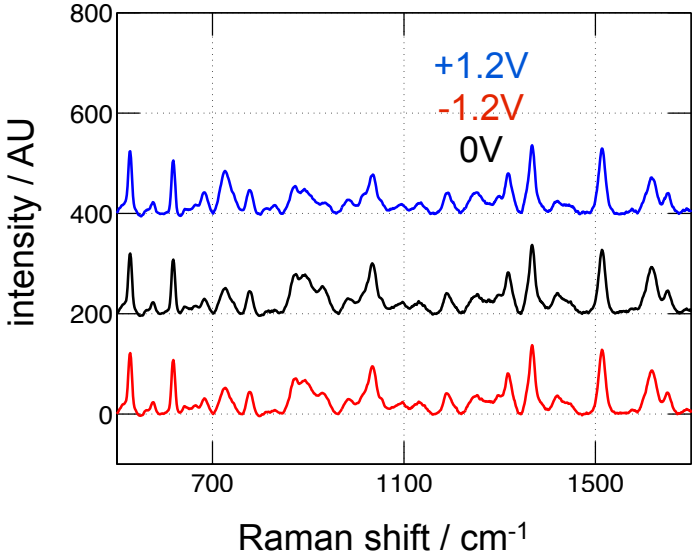

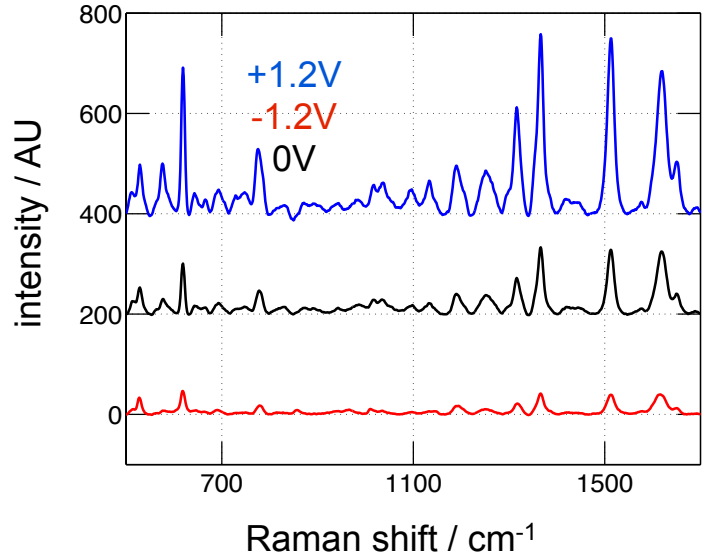

Simulation-Optimized Sequence

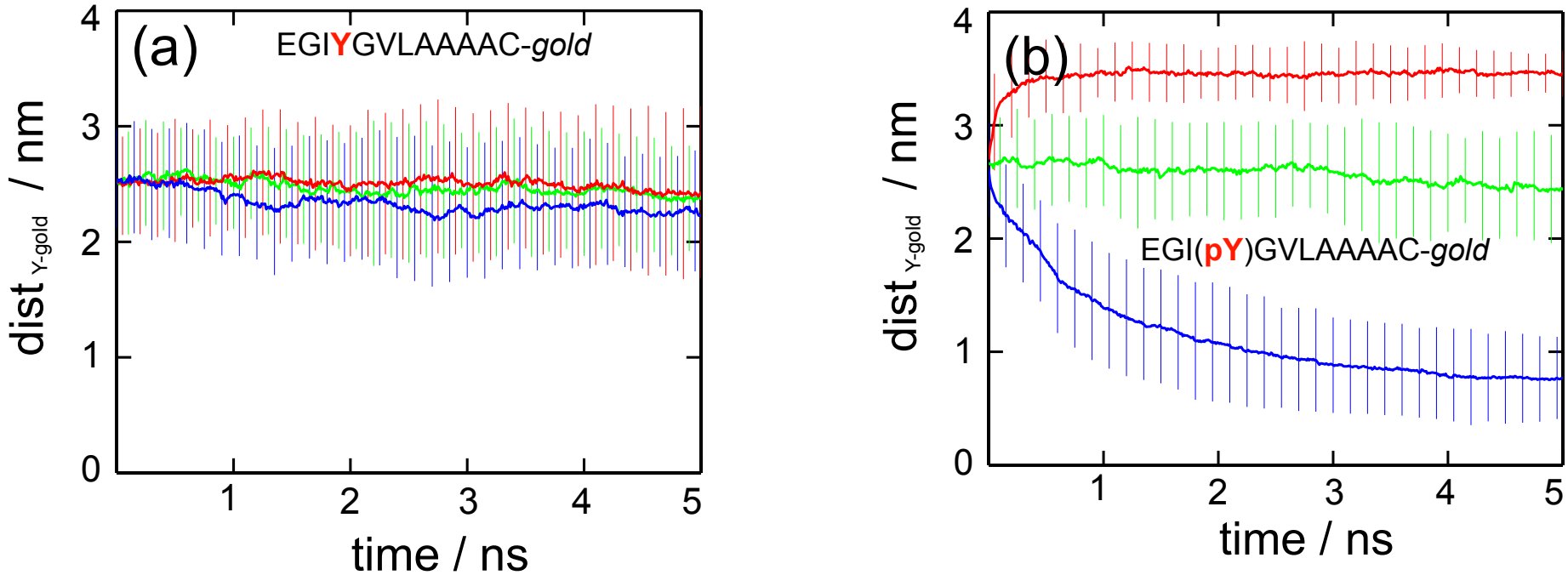

A new sequence is proposed from molecular dynamics simulations. There are no rhodamine caps, avoiding aggregation. Unnecessary lysine residues are changed to alanine residues. The resulting non-phosphorylated peptide sensor is still insensitive to an electric field, while the phosphorylated one is responsive to an external electric field; therefore the sensor should produce distinctive Raman signatures for opposite voltage polarities. Error bars represent standard deviation. Colors blue, red, and green represent +60 V, -60 V and 0 voltage biases.

Accuracy of the New Assay Method

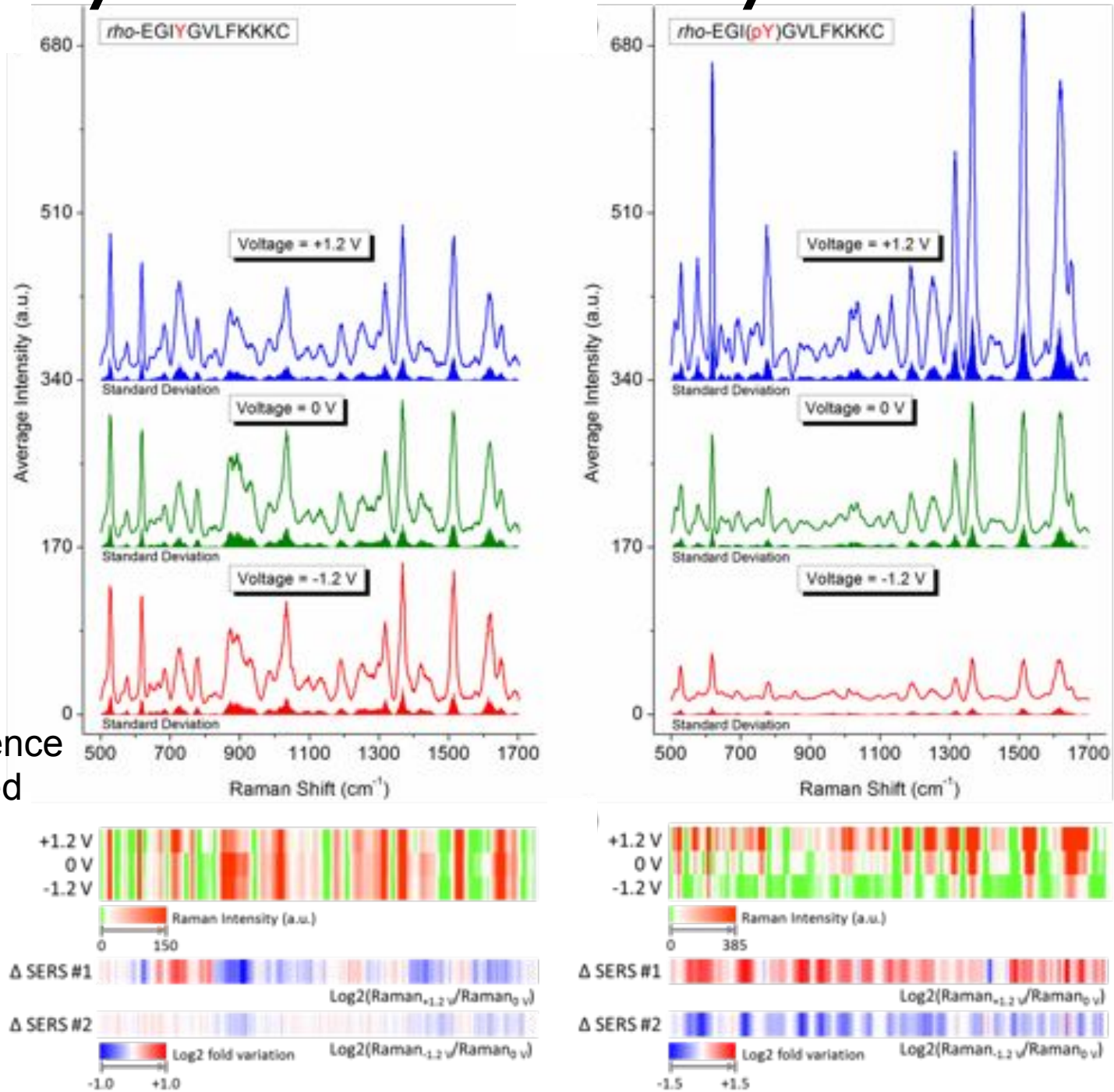

SERS spectra difference is amplified by applied electric field

Achievements Built on People

5 faculty members (2 physics, 1 chemistry, 1 biochemistry, 1 computer science);
8 developers; 1 system admin.; 16 post docs; 24 graduate students; 3 administrative staff

L. Kale, J. Phillips: NAMD
J. Stone, K. Vandivort: VMD
I. Solov'yov, D. Chandler, M. Sener, J. Strumpfer, J. Perilla, Y. Liu, J. Gumbart, Y. Chan, X. Zou, E. Cruz-Chu: Science Proj.

J. Frank, Columbia U.: MDFF, ribosome
R. Beckmann, U. Munich: ribosome
W. Baumeister, MPI: whole cell imaging
L. Liu, Greg Timp, UIUC, H. Gaub, U. Munich: biosensors; N. Hunter, Sheffield photosynthesis;.